Chapter V

Stability, Lipophilicity and Cytotoxicity

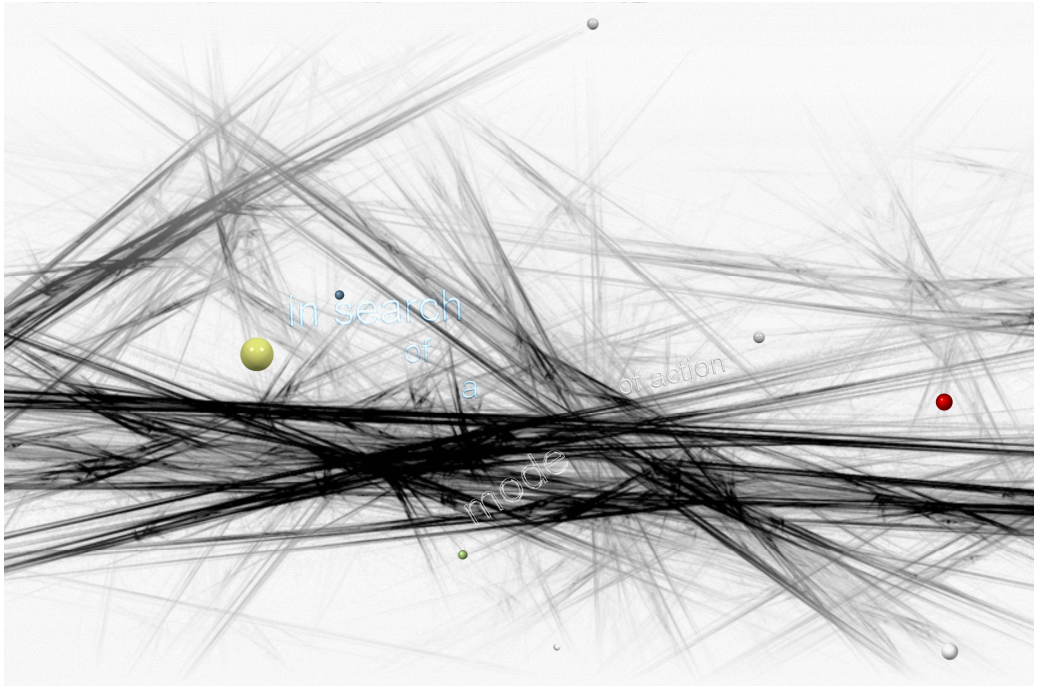

5.1 Stability

Stability requires a working definition tailored to the environmental characteristics important for assessing survival rates (Poole and Poole, 2003). Serum albumin, the most abundant protein in the blood stream (accounting for 60% of total plasma protein), is a major circulatory protein of known structure (Liu *et al.,* 2006). The diversity of chemical functions presented at the surface of the protein has multiple lipophilic binding sites, which may combine with hydrophobic substances like drugs especially neutral and negatively charged lipophilic compounds. Protein-binding plays an important role in pharmacokinetics and pharmacodynamics of the drug, because it affects both the activity of the drug and their disposition.

An important aspect has been to consider the stability of complexes under biologically relevant conditions (Berners-Price *et al.,* 1988). In general for metal complexes, there are likely to be a number of competing ligand exchange reactions that may lead to the breakdown of the complex in the external medium before it enters the cell. An active complex may not be that administered or tested *in vitro*; it may be transformed by ligand substitution and/or redox reactions before it reaches the target site (Berners-Price and ,Sadler, 1996). The distribution in such media is often impossible to calculate with any degree of certainty because not only are the appropriate thermodynamic and kinetic constants unknown, but the media are complex heterogenous mixtures of lipid components and aqueous solutions (Bell *et al.,* 1987).

Auranofin (1-thio-*β*-D-glucopyranose-2,3,4,6-tetraacetato-*S*) (triethylphosphine) gold(I) is active against intraperitoneally (ip) implanted P388 leukaemia mice (but only when administered ip) and it is inactive in other tumour models (Berners-Price *et al.,* 1990). This restricted range of activity may be related to facile ligand-exchange reactions which auranofin can undergo. In plasma and in cells, the tetraacetyl-*β*-D-thioglucose is readily displaced by other thiolate ligands, and the phosphine ligand can be released and undergo oxidation to the oxide. In contrast, *bis*-chelated Au(I) phosphine complexes related to $[Au(dppe)_2]^+$ are active against a spectrum of tumour models in mice (Berners-Price and Sadler, 1996). This

difference is likely to be related to the lower reactivity of the tetrahedral complexes, which can undergo ligand exchange reactions only by the chelate ring opening.

The ligand of $[Au(dppe)_2]Cl$, dppe, was shown to have *in vitro* cytotoxic properties in tumour cells and it was suggested that the toxic response was a consequence of the delivery of dppe to the appropriate biological target (Smith *et al.,* 1989). Additionally, this free diphosphine exhibits good anti-tumour activity in a similar range of animal models, but its potency is more than 25-fold lower than the gold complex (Berners-Price and Sadler, 1987b). Unfortunately, this phosphine is easily susceptible to air oxidation (Khokhar *et al.,* 1990). Replacement of the phenyl substituents by ethyls reduced both the cytotoxic potency and activity against P388 leukaemia (Berners-Price *et al.,* 1990). The compound $Et_2P(CH_2)_2PEt_2$ (depe) exhibits no anti-tumour activity and is relatively non-toxic to mice. This can be rationalised by the ease with which it (depe) undergoes oxidation in aqueous media in comparison with phenyl-substituted diphosphines, which in turn is related to the difference in autoxidation pathways for alkyls and aryl phosphines.

5.2 Nuclear Magnetic Resonance Spectroscopy (NMR)

NMR spectroscopy is a powerful method for investigating the speciation of metal complexes in solution and to a lesser extent in the solid state (Berners-Price and Sadler, 1996). Spin- ½ nuclei offer the most potential for the study of metallodrugs. ^{1}H NMR spectroscopy will continue to be the most widely used for investigating ligand behaviour and ^{31}P (100% abundance) with high sensitivity is invaluable for studies of metal phosphine drugs. ^{31}P NMR has shown that $[Au(dppe)_2]^+$ (unlike auranofin) remains essentially intact in human plasma and does not react significantly with glutathione or albumin. The results obtained suggest that the complex could be transported in plasma and transferred intact through membranes.

Recent ^{31}P NMR studies of tetrahedral bisphosphine Au(I) complexes with pyridyl substituents (R and R' are 2-pyridyl, 4-pyridyl) have also shown that these are

stable for at least 30 h when incubated in blood plasma at 37℃ (Berners-Price and Sadler, 1996). They are also kinetically stable and undergo slow exchange in the presence of a sodium salt of *β*-D-thioglucose. However, it must be noted that the concentrations of the complex employed in the studies are more than 100 times those of physiological relevance (Berners-Price and Sadler, 1987b). This was necessary on account of the relative insensitivity of NMR techniques.

5.3 Evaluation of stability of the test compounds by ^{31}P NMR spectroscopy.

In biological assays, DMSO, ethanol or H_2O are the solvents most commonly used to dissolve compounds and cell culture medium (supplemented with 10% foetal calf serum) is used to dilute the stock solution. *In vitro* assays involve incubation of cells with the compounds for a varied period of time (hours to days). The aim of carrying out these tests was to determine the stability of the test compounds before carrying out any biological work. ^{31}P NMR spectra of all the compounds contained one phosphorus peak and hence appearance of other (new) peaks was used to track any chemical changes.

5.4 Materials and methods

5.4.1 Reagents and compounds

- Analytical grade dimethylsulphoxide (DMSO)-Acros Organics-Belgium
- Deuterated DMSO-d_6 –Sigma Aldrich (Germany)
- Cell culture medium (EMEM supplemented with 10% foetal calf serum)
- Impure sample of $[Pt(d2pyrpe)_2]Cl_2$
- Test compounds (7) i.e, $[Pt(dppe)_2][PF_6]_2$ (**Pg 1**), $[Pd(dppe)_2][PF_6]_2$ (**Pg 3**), $[Pd(dppen)_2][PF_6]_2$ (**Pg 4a**), $[Pt(d2pyrpe)_2][PF_6]_2$ (**Pg 5**), $[Pt(d3pyrpe)_2][PF_6]_2$ (**Pg 6**), $[Pd(d2pyrpe)_2][PF_6]_2$ (**Pg 8**) and $[Au(dppe)_2]Cl$

5.4.2 General experimental procedure

Small amounts (~6 mg) of the test compounds were dissolved in DMSO, DMSO-d_6 and/or cell culture medium (EMEM). Immediate analysis with a NMR Bruker 300 spectrophotometer (121.5 MHz) was carried out. The samples were analysed at 0 h, 24 h and 7 days with incubation at 37°C between analyses.

5.5 Results

The first complex to be tested was an impure sample of $[Pt(d2pyrpe)_2]Cl_2$. Purification of this compound was unsuccessful due to decomposition and this precluded the synthesis of additional compounds with Cl^- as counterion. The crude sample which was a mixture of $[PtCl_2(d2pyrpe)]$ and $[Pt(d2pyrpe)_2]Cl_2$ (*Fig 5.1*) was treated as described in the general procedure.

Figure 5.1 shows the structures of the compounds in the impure sample while **Table 5.1** shows the ^{31}P chemical shifts changes.

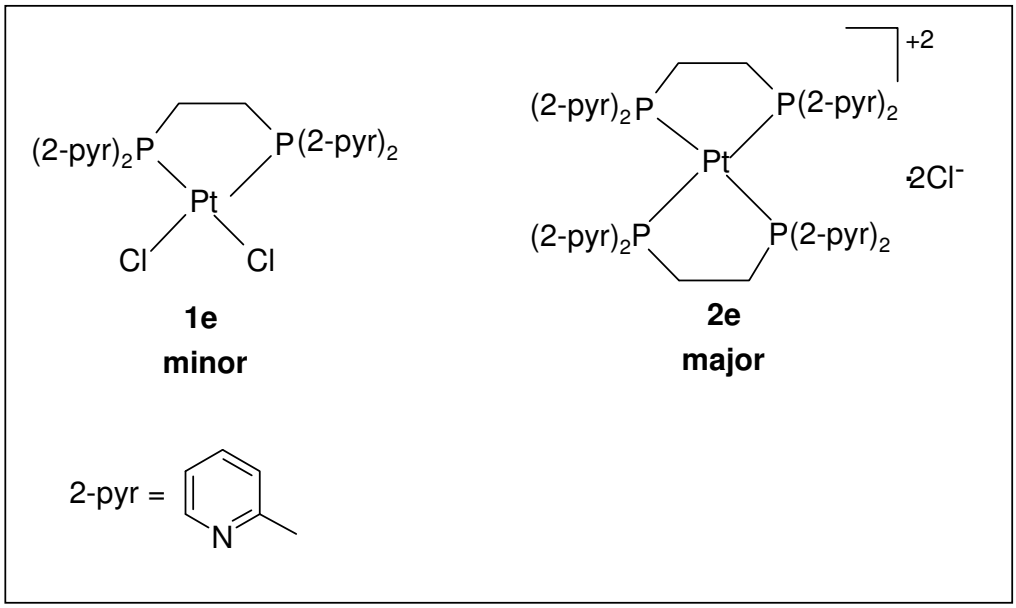

Figure 5.1: Mixture of $[PtCl_2(d2pyrpe)]$ (**1e**) and $[Pt(d2pyrpe)_2]Cl_2$ **(2e)**

Table 5.1: $^{31}P\{^{1}H\}$ NMR chemical shift changes of the mixture containing compound **1e** and **2e**

	DMSO	**EMEM**
0h	*55.1 #47.6	55.1 47.6
24h	47.6	47.6
7 days	47.6	55.1** 47.6**

*Major compound, $[Pt(d2pyrpe)_2]Cl_2$

Minor compound, $[PtCl_2(d2pyrpe)]$

** Equal intensity

Figures 5.2-5.4 depict the changes that occurred as seen from actual NMR spectra (DMSO) and 5.5-5.7 (EMEM).

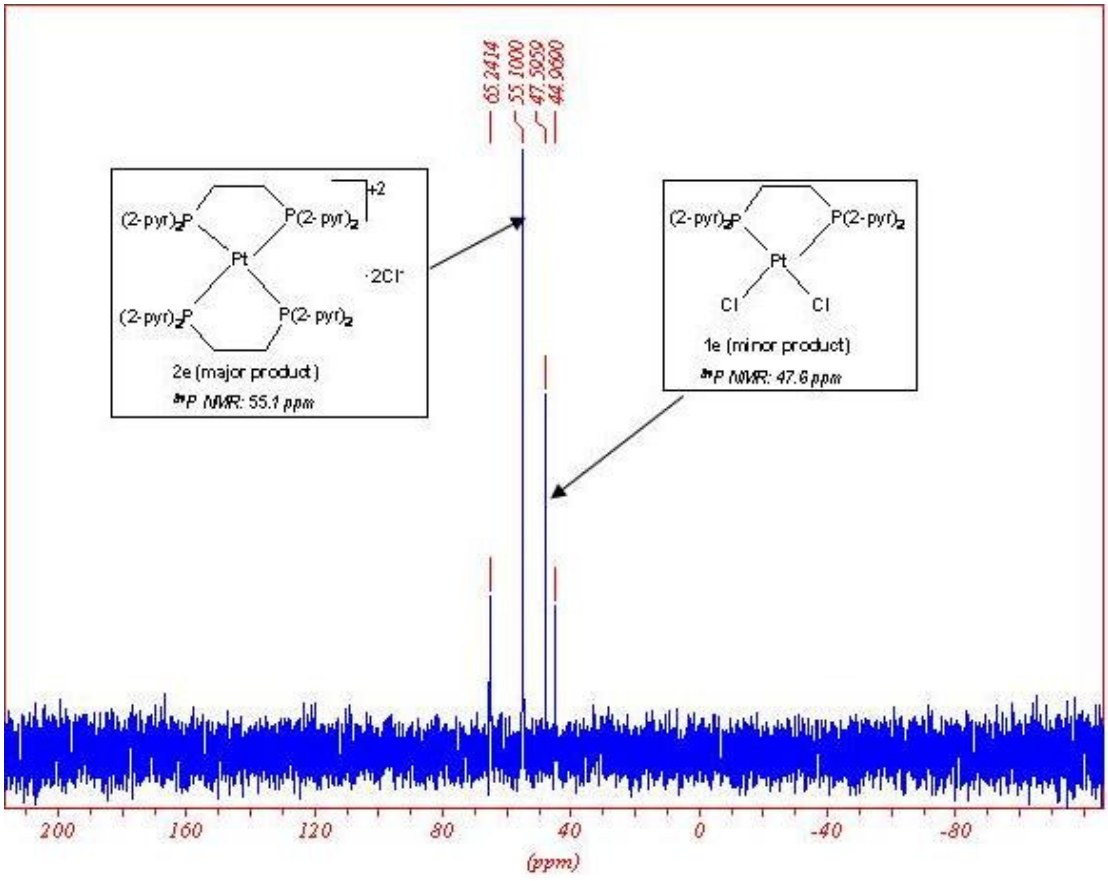

Fig 5.2: $^{31}P\{^{1}H\}$ NMR spectrum of the mixture at 0h in DMSO

The desired compound $[Pt(d2pyrpe)_2]Cl_2$ (**2e**) was not stable (*Table 5.1 and Figures 5.2-5.4*). At the beginning of the experiment, **2e** was the major complex in the mixture but it was replaced by the *mono*-chelated species, $[PtCl_2(d2pyrpe)]$ (**1c**) after 24h incubation in DMSO (*Fig 5.3*). These analyses demonstrated that purification of the compound was hindered by instability.

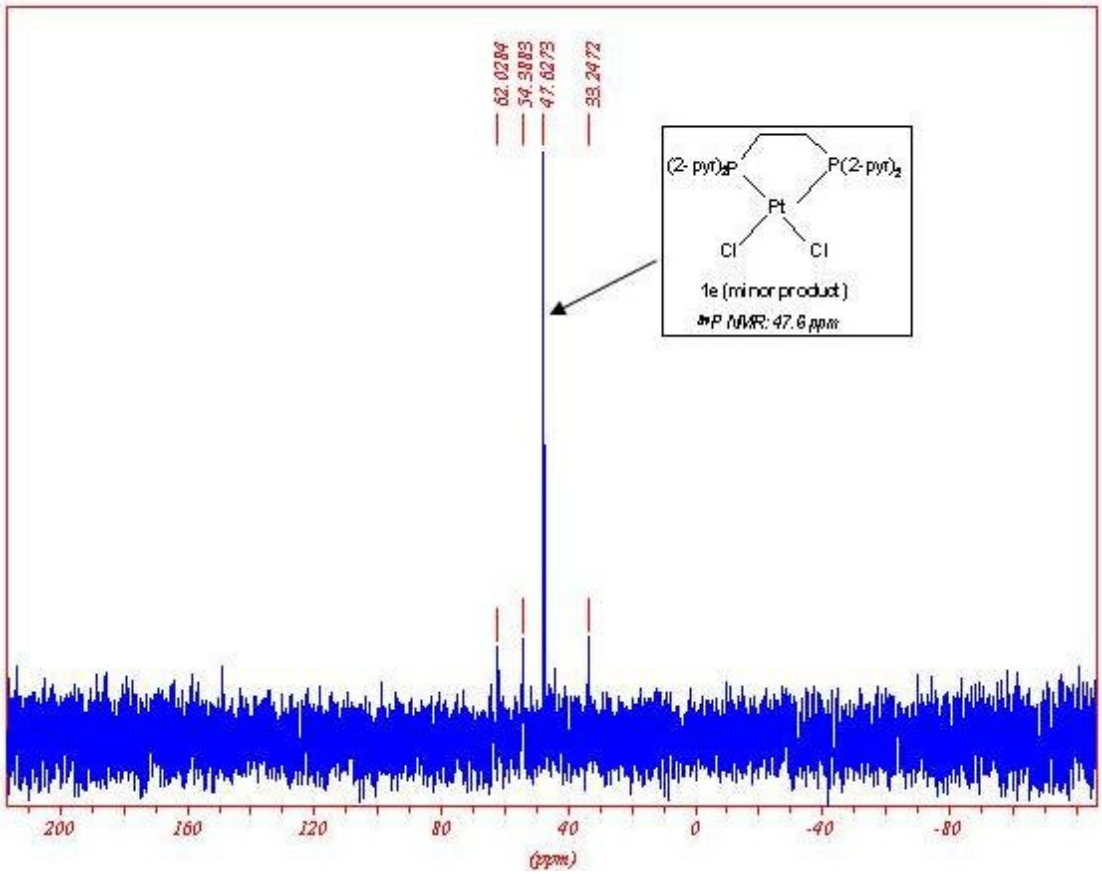

Fig 5.3: $^{31}P\{^{1}H\}$ NMR spectrum of the mixture after 24 h in DMSO

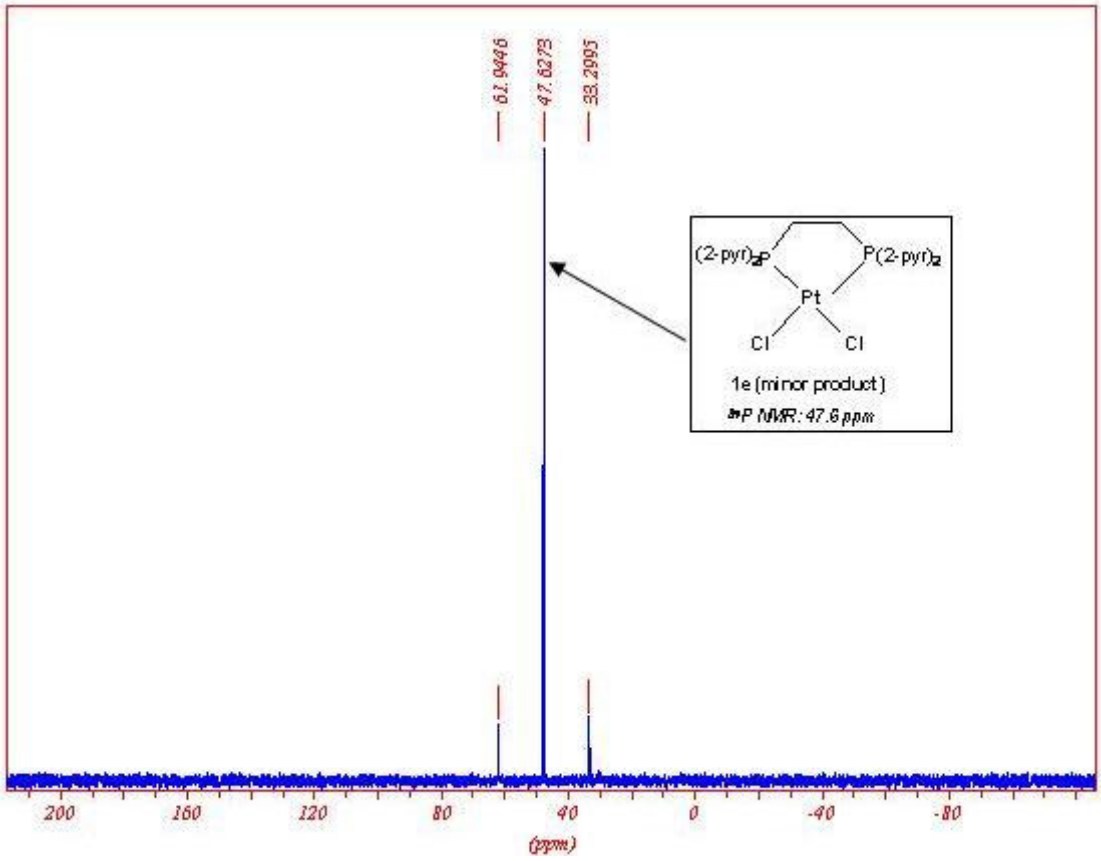

Fig 5.4: $^{31}P\{^{1}H\}$ NMR spectrum of the mixture after 7 days in DMSO

The sample in DMSO exhibited different behaviour from that dissolved in cell culture medium (*Table 5.1* and *Figures 5.5-5.7*). In DMSO, the mixture was converted to the *mono*-chelated complex **1e** and remained the same up to day 7. In contrast, the *mono*-chelated species (**1e**) (*Fig 5.6*) was converted back to the *bis*-chelated complex (**2e**) by day 7 (*Fig 5.7*). This last spectrum shows the two compounds existing in equal amounts at the end of the study.

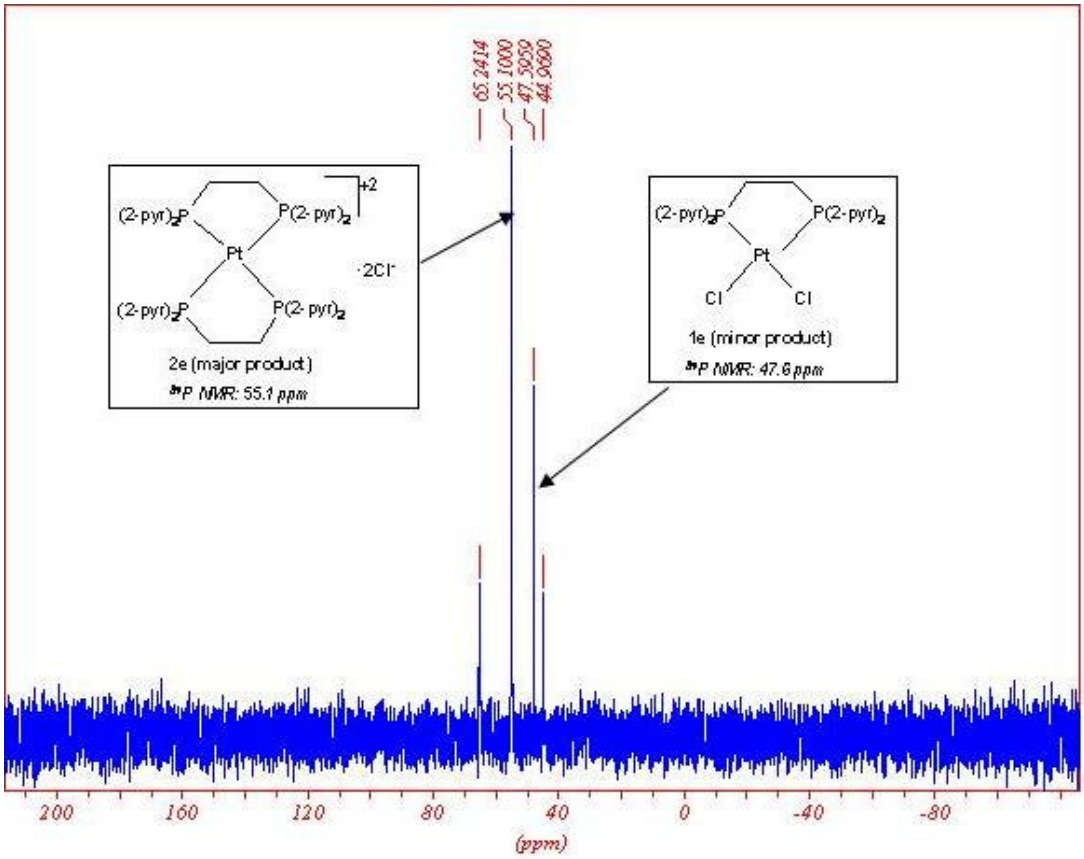

Fig 5.5: $^{31}P\{^{1}H\}$ NMR spectrum of the mixture at 0 h in EMEM

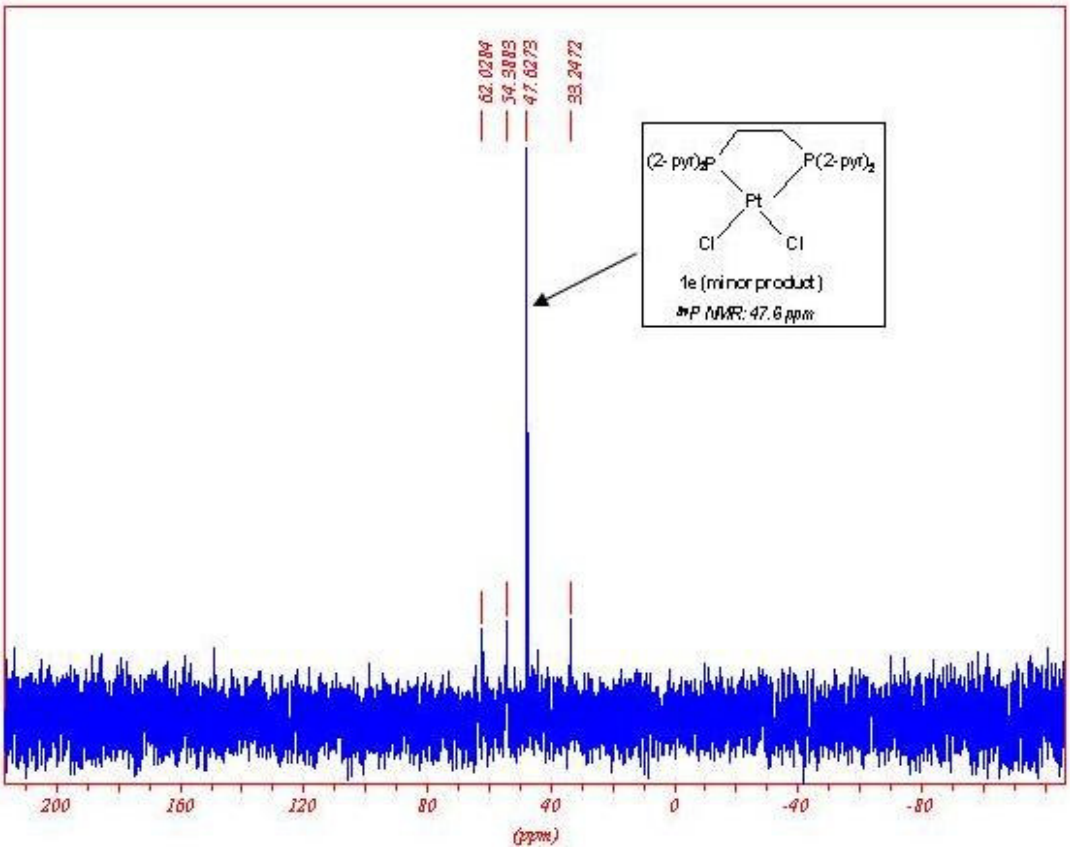

Fig 5.6: $^{31}P\{^{1}H\}$ NMR spectrum of the mixture after 24 h in EMEM

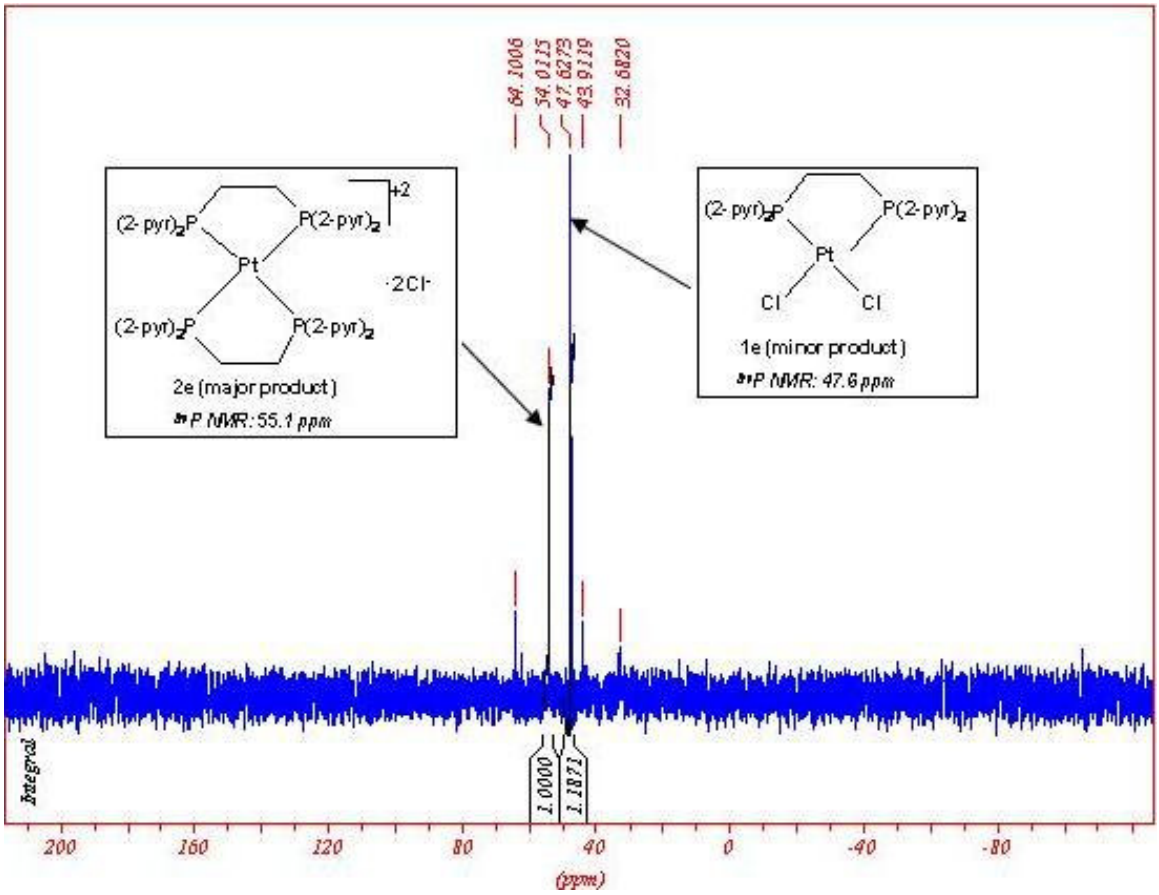

Fig 5.7: $^{31}P\{^{1}H\}$ NMR spectrum of the mixture after 7 days in EMEM

These stability tests validated the fact that the compounds with Cl^- as the counter-ion were labile and hence unsuitable for any biological work. Failure in purifying the compounds was also clarified by these tests. Replacement of the chlorides with BPh_4^- and/or PF_6^- led to stable and pure complexes. One of the complexes, $[Pt(d2pyrpe)_2][BPh_4]_2$ precipitated out in the presence of cell culture media and showed no toxicity against cells. This precluded the synthesis of similar compounds as possible candidates for anti-cancer application.

The compounds discussed in Chapters 3 and 4 were investigated for stability as described above. The results from ^{31}P NMR spectroscopy for the seven (7) compounds are tabulated below (Table 5.2).

Table 5.2: $^{31}P\{^{1}H\}$ NMR chemical shifts (ppm) of test compounds in DMSO and/or EMEM

Compound	**Chemical shift (0 h)**		**Chemical shift (24 h)**		**Chemical shift (7 days)**	
	DMSO	**EMEM**	**DMSO**	**EMEM**	**DMSO**	**EMEM**
Pg 1	49.4	49.3	49.4	49.6	49.4	No peak
Pg 3	58.1	58.0	58.1	58.1	58.1	36.8
Pg 4a	65.1	67.4	65.1	68.4 20.9	65.1	20.9
Pg 5	55.8	55.8	55.8	54.8	55.8	54.9 33.2
Pg 6	42.0	42.0	42.0	41.6 37.8	42.0	41.5 36.6 31.2
Pg 8	64.0	62.9	64.0	29.5	64.0	29.5
$[Au(dppe)_2]^+$	22.5	No peak	22.5	No peak	22.5	No peak

All the compounds were soluble in DMSO and no precipitation occurred throughout the experiment. In contrast, precipitation (negligible) of the test compounds occurred in the presence of cell culture medium (EMEM). Table 5.2 shows that the compounds dissolved in DMSO were stable throughout the experiment as the chemical shifts remained the same. The EMEM fraction exhibited large chemical shift changes during the course of the experiment (0h-7 days).

The platinum complexes (**Pg 5** and **Pg 6**) contained extra peaks at the end of the experiment but the original peaks were still present. In contrast, new peaks completely replaced the original peaks in the palladium complexes (**Pg 3, Pg 4a** and **Pg 8**). The new peaks (range of 20.9-36.8 ppm) can be attributed to oxidation products of the phosphine ligands in cell culture media. Autoxidation studies carried out on the ligand, dppe, showed that 65% of the ligand had oxidised (^{31}P = 32.8 ppm) after standing in $CDCl_3$ (deuterated chloroform) for 5 days (Berners-Price *et al.,* 1987a). Diphosphine dioxide with ^{31}P NMR chemical shifts of 31.2

and 38.5 (in methanol and dimethylacetamide, respectively) were observed. c*is*-dppen was the most stable diphosphine studied, no appreciable oxidation was observed after 2 days in $CDCl_3$, DMA or methanol.

The ^{31}P NMR signal for $[Au(dppe)_2]Cl$ in our studies could not be observed due to broadening of the peak. This could be as a result of a number of factors: for example, an exchange process with another species for which the ^{31}P resonance is too broad or too low in intensity to be resolved (Berners-Price and Sadler, 1987b). Studies of the above compound in plasma concluded that broadening could arise from an inhomogeneous distribution of the complex (within the plasma), chemical shift anisotropy, or a relative (on the NMR time scale) immobilisation of the complex through binding interactions. These could involve ion-pairing between the $[Au(dppe)_2]^+$ cation and negatively charged plasma components, or hydrophobic interactions involving the phenyl rings and lipophilic components of the plasma. In studies where cisplatin was incubated with Dulbecco's cell culture medium, the singlet for the S-methyl of L-methionine in the medium disappears and a new peak characteristic of Pt-bound L-Met appears (Berners-Price and Sadler, 1996).

5.6 Lipophilicity

Lipophilicity expressed as a ratio of octanol solubility to aqueous solubility appears in some form in almost every analysis of physico-chemical properties related to absorption (Lipinski *et al.,* 1997). If a third substance is added to a system of two immiscible liquids in equilibrium, the added component will distribute itself between the two liquid phases until the ratio of its concentrations in each phase attains a certain value: the distribution constant or partition coefficient (Berthod and Carda-Broch, 2004). Chemists and pharmacologists began to take an interest in partition coefficients at the turn of the 20th century (Albert, 1979). Their stimulus was the positive correlation that Overton and Meyer (1899) had demonstrated between the bio-depressant (e.g. hypnotic) action of many chemically unrelated substances, and their preference for the lipoid layer when partitioned between olive oil and water.

Combinatorial chemistry is able to produce large numbers of new compounds that could be potential drugs (Berthod and Carda-Broch, 2004). A drug has to cross four barriers associated with absorption, distribution, metabolism and excretion referred to ADME interface. The core properties required to estimate absorption, distribution, and transport in biological systems are solubility, stability, and acid-base character (Poole and Poole, 2003). These properties are used directly or through structure-activity relationships to help design active compounds and determine toxicity and membrane permeation. The 1-octanol-water partition coefficient (log*P*) is widely used in quantitative structure-activity relationships/quantitative structure-property relationship (QSAR/QSPR) approaches (Molnár *et al.*, 2004).

5.6.1 Relationship between lipophilicity and activity

Octanol/water partitioning has been shown to correlate with serum protein binding and is also suited for modelling lipophilic interactions with membranes that have high amounts of proteins incorporated (Hartmann and Schmitt, 2004). Lipophilicity can be an important determinant of activity because passive uptake across the lipid bilayer making up the cell membrane is facilitated by higher lipophilicity (Hambley, 1997). The biodistribution, protein binding, and metabolism of drugs may be altered by their lipophilicity (Poole and Poole, 2003). It is generally held that lipophilic compounds are preferred targets for metabolism, often leading to high clearance rates and frequently, lipophilicity correlates positively with a high protein binding. Changes in drug lipophilicity appear to alter host toxicity associated with non-specific binding and renal drug elimination (McKeage *et al.,* 2000). Compounds that can be delivered at high doses are expected to prove more active because of the dependence of activity on tumour drug concentration *in vitro* and *in vivo* models.

One of the most reliable methods in medicinal chemistry to improve *in vitro* activity is to incorporate properly positioned lipophilic groups (Lipinski *et al.,* 1997). The hydrophilic character of metal ions can be changed by conjugation with organic compounds (Zimmermann *et al.,* 2003). This process is often found in nature to enhance or impede the transfers of metals through the cell membrane. The use of

aromatic cations (also known as lipophilic cations) as anti-cancer agents has had a long history (McKeage *et al.,* 2000). Strongly positively charged terephthalanilide derivatives were developed for clinical trials over 30 years ago, but were abandoned because of toxicity. Bisquaternary derivatives of the above compound were synthesised in an approach to controlling drug lipophilicity and many showed excellent activity against the transplantable L1210 leukaemia in mice.

5.7 Aim of the experiment

The experiment described below aimed at determining lipophilicity (Log *P*) of each compound and correlating it to cytotoxicity and selectivity.

5.8 Materials and methods

5.8.1 Reagents and compounds

- Analytical grade *n*-octanol (Sigma-Aldrich, Germany)
- Distilled water
- Test compounds (7) i.e, $[Pt(dppe)_2][PF_6]_2$ (**Pg 1**), $[Pd(dppe)_2][PF_6]_2$ (**Pg 3**), $[Pd(dppen)_2][PF_6]_2$ (**Pg 4a**), $[Pt(d2pyrpe)_2][PF_6]_2$ (**Pg 5**), $[Pt(d3pyrpe)_2][PF_6]_2$ (**Pg 6**), $[Pd(d2pyrpe)_2][PF_6]_2$ (**Pg 8**) and $[Au(dppe)_2]Cl$

5.8.2 General procedure for determination of lipophilicity

A volume of water-saturated octanol and a volume of octanol-saturated water were prepared by shaking equal volumes of octanol and water for 15 min and then allowing the layers to separate overnight in a separating funnel (Bowen, 1999). The two fractions were collected separately being careful not to allow cross contamination of one solvent layer onto the other. Hereafter, the octanol will refer to distilled water-saturated octanol and water will refer to as octanol-saturated distilled water. 60 μM octanol stock solutions of the complexes were prepared followed by preparation of 40 μM and 20 μM solutions by further dilution with octanol, so that the final volumes were 5 ml.

Each of these solutions was analysed separately by U.V-visible spectroscopy to give an absorbance maxima at a wavelength *ca* 251 and 298 nm. This absorbance corresponded to the Ci value (initial concentration) for each solution. 5 ml of water was added to each of these solutions to make up a final volume of 10 ml. Each of the solutions was shaken vigorously and then independently transferred to separating funnels. Separation of the aqueous extract from the octanol took place after the two phases settled over periods between 30 min to 15 hours. Analysis of this extract by UV-visible spectroscopy gave absorbance maxima at a wavelength identified from the Ci determination. This absorbance corresponded to Cw (concentration in water) value for each solution. Ci-Cw established the concentration of each complex remaining in the octanol layer, Co. Partition coefficient (log *P*) defined as the logarithmic ratio of compound concentrations in the organic and aqueous phases (log Co/Cw) (McKeage *et al.,* 2000) was then calculated.

5.8.3 Statistical analysis

The experiment was performed three times and results (*Fig 5.8*) are an average of triplicate values (±SEM).

5.9 Results and discussion

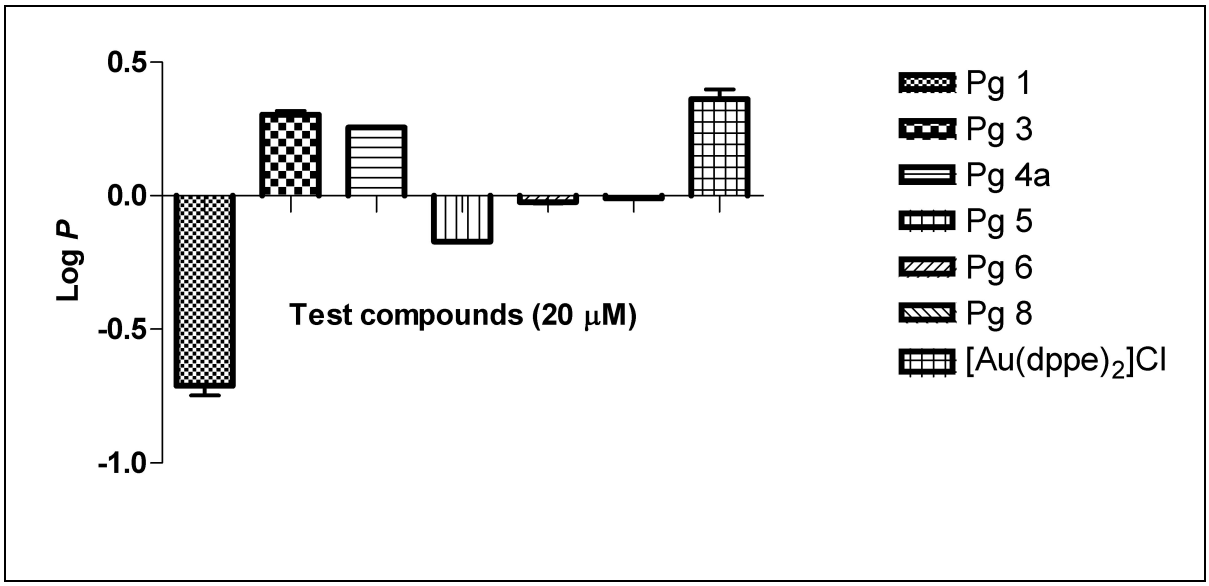

Fig 5.8: Log *P* values of the test compounds at 20 μM. Positive values indicate more lipophilic character while negative values point towards less lipophilic character.

With the exception of **Pg 1**, all the complexes with phenyl groups, **Pg 3, Pg 4a** and [Au(dppe)$_2$]Cl showed lipophilic character (positive values). [Au(dppe)$_2$]Cl showed the greatest lipophilic character (log *P* = 0.362) followed by **Pg 3a** (log *P* = 0.303) and **Pg 4a** (log *P* = 0.256). As expected, complexes with pyridyl groups (**Pg 5**, **Pg 6**, **Pg 8**) had negative log *P* values, indicating less lipophilic character (more hydrophilicity). The platinum pyridyl complexes **Pg 5** and **Pg 6** (which differ by the position of the N in the pyridyl ring) showed hydrophilic character with the former being more hydrophilic (Log *P* =-0.172) than the latter (Log *P* = -0.024). The degree of hydrophilicity depends critically on the presence of the pyridyl ligand and on the position of the N atom (McKeage *et al.,* 2000).

Practical considerations are important in the determination of octanol-water partition coefficients using the above procedure (Poole and Poole, 2003).

- Complete separation of the layers is important as any droplets of octanol in the aqueous phase may contain large amounts of sample;
- Pre-saturation of the two phases is required;
- The sample concentration must be less than the critical micelle concentration;
- Measurements need to be carried out at concentrations below the aqueous solubility limit and;
- Lipophilic basic compounds may adsorb onto surface of the apparatus.

The unexpected results from **Pg 1** (log *P* = -0.710) may have been as a result of an interface that formed between octanol and water. There is a possibility that some of the precipitated compound was collected into the water phase during separation. At 60 µM, it had a log *P* value of 0.222 which indicated that a larger portion of the compound partitioned into the octanol phase at higher concentration. This trend was seen in the standard, [Au(dppe)$_2$]Cl which had a log *P* value of 1.036 at 60 µM vs 0.362 at 20 µM. Future developments will probably include less dependence on Log *P* as a single descriptor for property estimations in favour of a suite of models tailored to individual distribution and transport properties based on the solvation parameter model (Poole and Poole, 2003).

5.10 Cytotoxicity

Understanding both the thermodynamics and kinetics of metal speciation is crucial to the advancement of inorganic molecular pharmacology (Berners-Price and Sadler, 1996) and the establishment of structure-activity relationships is an important part of the drug design process. One of the biggest challenges lies in the control of the toxicities of metal compounds and hence understanding the species which are responsible. The roles played by the intact metal complex itself and either the metal or its ligands separately must be considered. In a series of Pt(II) and Pt(IV) complexes with *cis* chloro and *cis* substituted amine ligands, the role of solubility and lipophilicity was considered in relation to toxicity (Hambley, 1997). For complex 5.9, it emerged that equal solubility in water and lipids correlated with minimum toxicity and maximum therapeutic index but maximum activity was observed with maximum solubility.

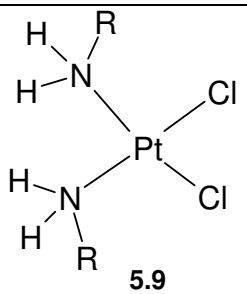

5.9

The ongoing challenge of this work has been to find a molecule with suitable pharmacological properties-high solubility, high stability, low toxicity and favourable pharmacokinetics-for use in humans (Don and Hogg, 2004).

[Au(d2pyrpe)$_2$] was shown to be toxic to B16 melanoma while its analogue [Au(d4pyrpe)$_2$]Cl was inactive (Berners-Price *et al.,* 1990). Additional experiments on human blood confirmed that the 2-pyridyl complex readily partitioned between plasma and red cells while the 4-pyridyl complex was retained in the blood plasma fraction (Berners-Price and Sadler, 1996).

5.11 Determination of cytotoxicity

Cytotoxicity assays were performed on cell cultures to evaluate the level of sensitivity of cancer cells and normal healthy cells to the experimental compounds. The aim of this assay was to correlate cytotoxicity to structure (metal or ligand) as well as lipophilicity. Additionally, it was used to select the most potent and selective compound(s) for further biological assays.

5.12 Materials and methods

5.12.1 Reagents and compounds

- Supplemented cell culture medium – Cell culture medium with 10% foetal calf serum (FCS).
- Phosphate buffered saline (PBS).
- DMSO (Sigma-Aldrich, Germany)
- MTT [3-(4,5-dimethylthiazol-2-yl)-2,5-diphenyl tetrazolium bromide] (Sigma Diagnostics Inc)
- Phytohaemagglutinin (PHA)
- Test compounds (7) - dissolved in DMSO (20 mM) and diluted in cell culture medium.

5.12.2 Cell lines and culture

Various human and murine cancer cell lines (sources are indicated in parentheses) were grown as monolayer cultures at 37℃ in 5% CO_2 in appropriate tissue culture medium (indicated in parentheses) supplemented with 10% v/v heat-inactivated serum (FCS) and 1% penicillin-streptomycin.

The following cancerous cell lines were used:

- HeLa- human adenocarcinoma of the cervix (ATCC) (EMEM)
- A2780- human ovarian cancer (EACC) (RPMI)
- A2780-cis- human ovarian cancer-cisplatin resistant (EACC) (RPMI)
- MCF-7- human breast cancer (ATCC) (DMEM)

- CoLo 320 DM- human colon cancer (ATCC) (RPMI)
- DU 145- human prostate cancer (ATCC) (RPMI)
- Jurkat- human T-cell line (NRBM) (RPMI)
- Novikoff- rat hepatocellular cancer (DKFZ) (RPMI)
- B16- mouse melanoma (ATCC) (RPMI)

Normal cells included:

- Human lymphocytes (resting and PHA stimulated)- fresh venous blood was obtained from healthy volunteers followed by isolation of lymphocytes (Anderson *et al.,* 1993).
- Chicken embryo fibroblasts- cells were isolated from chicken embryos (Freshney, 2005).
- Porcine hepatocytes- obtained from the Bio-artificial liver project under the supervision of Dr S. van der Merwe, Department of Internal Medicine, University of Pretoria (Fruhauf *et al.,* 2004).

5.12.3 Sample preparation

All the complexes were dissolved in DMSO to give a stock concentration of 20 mM (stored at -70℃). Immediately before the cell experiments, the stock solution was diluted in appropriate growth medium (containing 10% FCS) to give final DMSO concentrations not exceeding 0.5% and drug concentrations of 0.003-100 µM.

5.13 General procedure

The assays were performed using a metabolic assay based on the reactivity of MTT [3-(4,5-dimethylthiazol-2-yl)-2,5-diphenyl tetrazolium bromide] (Mosmann, 1983; Meyer *et al.,* 2005). MTT is a pale yellow substance that is metabolised to dark blue formazan crystals by metabolically active cells. The amount of formazan produced is directly proportional to the amount of cells over a wide range.

80 µl of medium (60 µl in the case of the lymphocytes earmarked to be stimulated) was dispensed into each well of a 96 well tissue culture plate (micro-titer plate).

100 µl of cell suspension (2 x 10^4 – 2 x 10^6 cells/ml/well depending on the cell type) was added and then allowed to incubate for 1 hour at 37ºC in an atmosphere of 5% CO_2. 20 µl of the experimental drug (eight varying concentrations) was added in triplicate to the wells. However, control wells received 20 µl of growth medium instead of the experimental drug. Lymphocytes earmarked to be stimulated received 20 µl PHA 5 minutes after the addition of the drug.

After the incubation period (3 and 7 days for lymphocytes and cancerous cells respectively), 20 µl MTT (5 mg/ml) was added to each well and cultures were incubated for 4 hours. Cells were then centrifuged for 10 min at 2000 rpm (800 g) (Beckman TJ 6 centrifuge) and the supernatant removed without disturbing the pellet. The cells were washed with 150 µl PBS (per well) and centrifuged for 10 min at 2000 rpm (800 g) (Beckman TJ 6 centrifuge). The supernatant was removed and plates were left to dry in the dark. 100 µl DMSO was added to each well to solubilise the formazan crystals and the plates were shaken for 2-4 hours. Culture plates were read on a plate reader using a wavelength of 570 nm and a reference wavelength of 630 nm.

5.14 Statistical analysis

Percentage survival (percentage of the relevant untreated control systems) was calculated and this value was used to determine the IC_{50} value (IC_{50} = the concentration (µM) of the experimental compound inducing a 50% decrease in cell growth).

5.15 Results and discussion

Table 5.3: IC_{50} values (µM) and S.E.M (±) of 7 compounds on various cancer cell lines as well as normal cells. The values are presented as a mean of three experiments carried out in triplicate.

	Pg 1	Pg 3	Pg 4a	Pg 5	Pg 6	Pg 8	$[Au(dppe)_2]Cl$
Hela	> 50	4.985 ± 0.367	5.467 ± 0.505	> 50	> 50	**0.638 ± 0.054**	0.288 ± 0.009
A2780	> 50	**0.707 ± 0.053**	**0.147 ± 0.015**	6.119 ± 0.283	17.501 ± 2.909	**0.974 ± 0.203**	0.011
A2780-cis	> 50	> 50	5.054 ± 0.703	> 50	> 50	**2.029 ± 0.273**	0.494 ± 0.043
MCF-7	> 50	18.087 ± 3.059	**2.873 ± 0.235**	> 50	> 50	**2.520 ± 0.219**	0.585 ± 0.010
Jurkat	> 50	3.598 ± 0.569	**1.445 ± 0.130**	37.704 ± 1.808	> 50	**0.711 ± 0.005**	0.131 ± 0.012
CoLo	> 50	13.257 ± 0.224	5.341 ± 0.374	13.803 ± 1.225	19.590 ± 1.172	**1.723 ± 0.021**	0.914 ± 0.028
DU145	**1.350 ± 0.315**	**0.253 ± 0.024**	**0.299 ± 0.001**	**2.485 ± 0.087**	**9.380 ± 0.448**	**0.541 ± 0.046**	0.007 ± 0.002
Resting lymphocytes	> 100	> 100	> 100	> 100	> 100	**> 100**	0.903 ± 0.041
Stimulated lymphocytes	> 100	> 100	> 100	> 100	> 100	**> 100**	0.182 ± 0.032

In general, the platinum complexes were less toxic than the palladium ones with **Pg 1** being the least toxic compound followed by **Pg 6** and **Pg 5** (*Table 5.3*). **Pg 8** was the most toxic of the palladium complexes followed by **Pg 4a** and **Pg 3**. With regard to all the novel complexes, prostate cancer (DU-145) was the most sensitive cell line (IC_{50} values of 0.253-9.380 µM) while ovarian cancer-cisplatin resistant cell line (A2780-cis) was the most resistant (IC_{50} values of 2.029-> 50 µM). Human ovarian cancer cell line- cisplatin sensitive (A2780) was sensitive to all the palladium complexes with IC_{50} values of 0.617 µM (**Pg 3**), 0.136 µM (**Pg 4a**) and 0.974 µM (**Pg 8**). Overall, **Pg 8** was the most toxic (over the whole range of cells) of the novel compounds followed by **Pg 4a** which showed comparative activity against Jurkat and MCF-7 cell lines.

$[Au(dppe)_2]Cl$ was more toxic than the novel compounds (*Table 5.3*). However, it exhibited non-selectivity as it was also toxic to both resting (IC_{50} = 0.903 µM) and

stimulated lymphocytes (IC_{50} = 0.182 µM) while the experimental compounds were not toxic even at a concentration of 100 µM.

Table 5.4: Cytotoxicity data of test compounds tabulated in order of increasing lipophilicity

Compound and Log P	**Pg 5 -0.172**	**Pg 6 -0.024**	**Pg 8 -0.009**	**Pg 4a 0.256**	**Pg 3 0.303**	**[Au(dppe)$_2$]Cl 0.362**
Hela	> 50	> 50	**0.638 ± 0.054**	5.467 ± 0.505	4.985 ± 0.367	0.288 ± 0.009
A2780	6.119 ± 0.283	17.501 ± 2.909	**0.974 ± 0.203**	0.147 ± 0.015	0.707 ± 0.053	0.011
A2780-cis	> 50	> 50	**2.029 ± 0.273**	5.054 ± 0.703	> 50	0.494 ± 0.043
MCF-7	> 50	> 50	**2.520 ± 0.219**	2.873 ± 0.235	18.087 ± 3.059	0.585 ± 0.010
Jurkat	37.704 ± 1.808	> 50	**0.711 ± 0.005**	1.445 ± 0.130	3.598 ± 0.569	0.131 ± 0.012
CoLo	13.803 ± 1.225	19.590 ± 1.172	**1.723 ± 0.021**	5.341 ± 0.374	13.257 ± 0.224	0.914 ± 0.028
DU145	2.485 ± 0.087	9.380 ± 0.448	**0.541 ± 0.046**	0.299 ± 0.001	0.253 ± 0.024	0.007 ± 0.002
Resting lymphocytes	> 100	> 100	**> 100**	> 100	> 100	0.903 ± 0.041
Stimulated lymphocytes	> 100	> 100	**> 100**	> 100	> 100	0.182 ± 0.032

Non-specific toxicity is expected to correlate with a compound's propensity to accumulate in cell membranes and therefore, its lipophilicity (Poole and Poole, 2003). [Au(dppe)$_2$]Cl was shown (*Fig 5.8*) to be the most lipophilic compound (log *P* = 0.362) of the experimental compounds and as expected, the most toxic (*Table 5.4*). Research has shown that there is a relationship between octanol-water partition coefficient and cytotoxic potency against human ovarian tumour cells (Berners-Price *et al.,* 1999a). There is a general increase in potency with increase in lipophilicity.

In the results presented in Table 5.4, one has to consider the role of different metals in interpretation of the data. The more hydrophilic compounds (**Pg 5** and **Pg 6**) were far less toxic than the lipophilic ones (**Pg 3** and **Pg 4a**). **Pg 8**, with intermediate lipophilicity was the most toxic of the novel compounds and hence

expected to show high selectivity. Studies have shown that the 2-pyridyl complexes of Ag(I) and Au(I) were cytotoxic to human ovarian cancer (JAM, CI-80-13S), cervical tumour (HeLa) and melanoma (MM96) cell lines (Bowen, 1999).

Pg 4a, **Pg 8** and $[Au(dppe)_2]Cl$ were tested on murine cancer cell lines as well as on normal cells (*Table 5.5*).

Table 5.5: IC_{50} values (µM) of **Pg 4a**, **Pg 8** and the standard $[Au(dppe)_2]Cl$ on murine cancer cell lines as well normal cells. The values are presented as a mean of three experiments carried out in triplicate.

	Pg 4a	**Pg 8**	**$[Au(dppe)_2]Cl$**
B16	0.872 ± 0.028	0.983 ± 0.035	0.0148 ± 0.0001
Novikoff	6.917 ± 0.394	0.654 ± 0.011	0.073 ± 0.002
Porcine hepatocytes	31.080 ± 5.320	1.755 ± 0.234	0.165 ± 0.026
Chicken embryo fibroblasts	2.379 ± 0.405	0.812 ± 0.037	0.220 ± 0.024

As seen previously (*Table 5.3*), $[Au(dppe)_2]Cl$ showed high potency and non-selectivity. **Pg 4a** was the most selective with IC_{50} values of 31.08 and 2.379 µM in porcine hepatocytes and chicken embryo fibroblasts, respectively. **Pg 8** gave comparable IC_{50} values in all the cells with the lowest being 0.654 µM (Novikoff) and the highest being 1.755 µM (porcine hepatocytes).

$[Ag(dppe)_2]NO_3$ were highly cytotoxic to B16 melanoma cells *in vitro* with an IC_{50} value of 4 µM (2 h exposure) while $[Au(dppe)_2]Cl$ had a value of 4.5 µM (Berners-Price *et al.,* 1988). Activity was retained when Au(I) was substituted by Ag(I) and Cu(I) as they possessed similar kinetic lability of the M-P bonds (Berners-Price and Sadler, 1996). In the current study, comparative compounds $[Pt(dppe)_2][PF_6]_2$ (**Pg 1**) and $[Pd(dppe)_2][PF_6]_2$ (**Pg 3**) displayed different anti-tumour behaviour. While the platinum complex was only active in prostate cancer cell line, the palladium analogue showed activity in all the cancer cell lines except A2780-cis. The high thermodynamic stability and high kinetic lability make palladium(II)

chelates more suitable for interacting with cancer cells and destroying them (Ali *et al.,* 2002).

$[Pd(d2pyrpe)_2][PF_6]_2$ (**Pg 8**) was selected for further tests in an effort to elucidate its mechanism of action. It was selected due the fact that it showed greater toxicity to more cancer lines than the rest of the experimental compounds. $[Au(dppe)_2]Cl$ was included in these investigations as a standard. Jurkat cells were used for the remainder of the assays as they could be compared to lymphocytes.

Chapter VI

Analysis of mitochondrial function

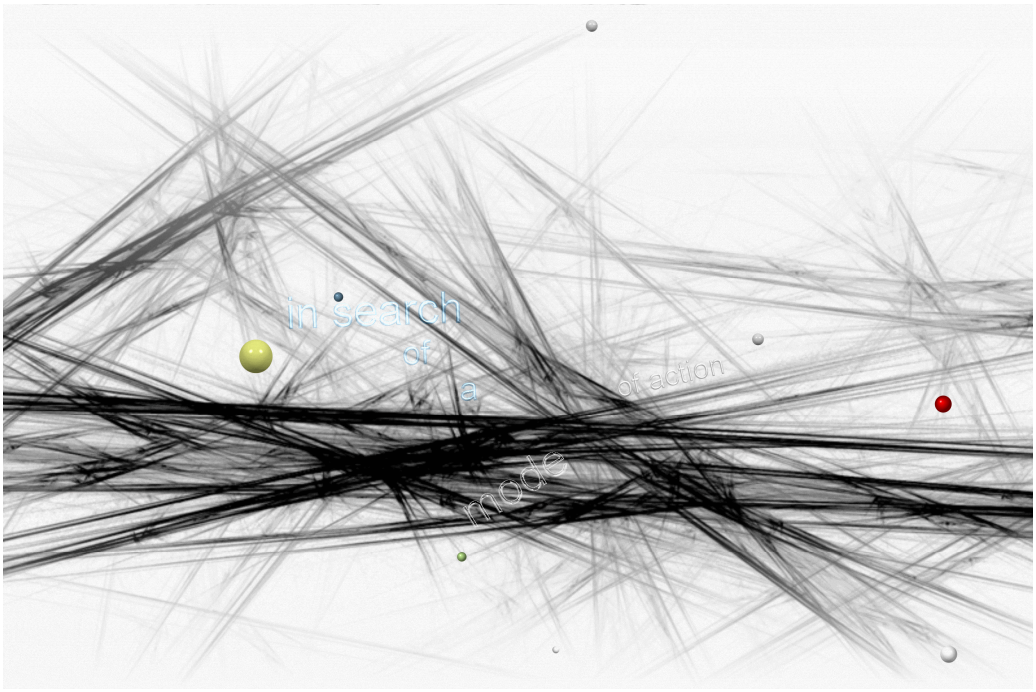

6.1 The Mitochondria

During the period 1900-1930, most cytologists recognised the mitochondrion as a well-defined and ubiquitous organelle, although at that time there was no agreement about its function (Modica-Napolitano and Singh, 2002). The identification of mitochondria as centres of energy metabolism came at the heels of refinements in cell fractionation techniques during the late 1940s, which allowed the successful separation of relatively pure, functionally intact mitochondria from other cellular components in liver cell homogenates. Mitochondria are involved in many of the normal processes occurring in living cells such as ATP synthesis, oxidative phosphorylation, calcium uptake and release, production of NADPH, pH control, synthesis of DNA, the tricarboxylic acid cycle and β-oxidation pathway (McKeage *et al.,* 2002).

In mitochondria, NADH and $FADH_2$, reducing equivalents derived from the degradation of food substrates donate electrons to oxygen, the final electron acceptor, and the energy released during this process is used to pump protons from the mitochondrial matrix to the intermembrane space (Schrauwen *et al.,* 2006) (*Fig 6.1*). As a result, an electrochemical gradient is created across the inner mitochondrial membrane. The exported protons flow back into the mitochondrial matrix through the F_0-F_{-1}-ATPase and the energy generated is used to synthesise ATP from ADP and inorganic phosphate (Pi).

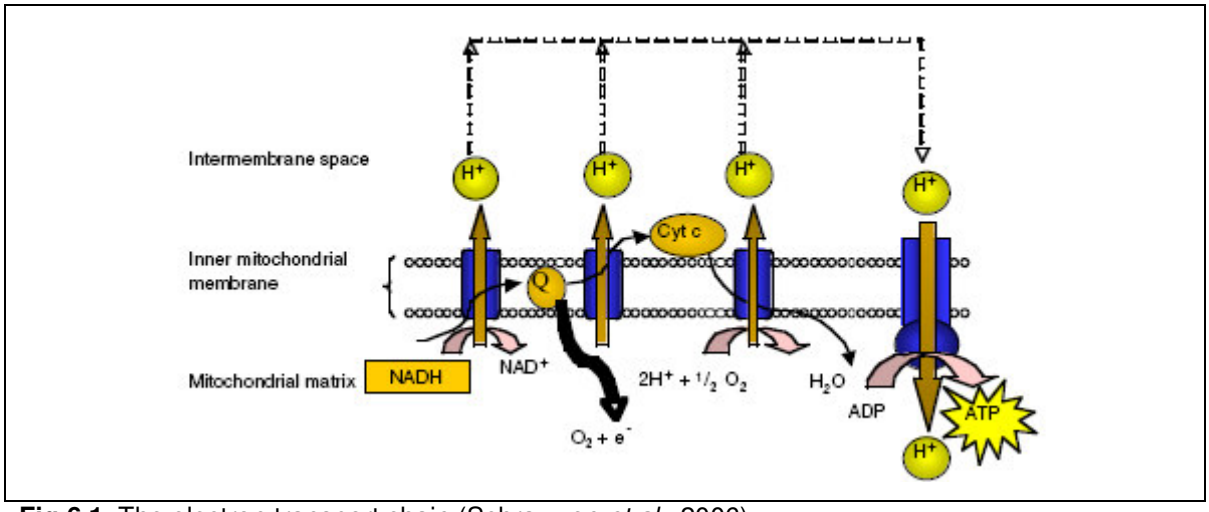

Fig 6.1: The electron transport chain (Schrauwen *et al.,* 2006).

The mitochondrial membrane potential, in situ, $\Delta\Psi_m$, is a sensitive indicator for the energetic state of the mitochondria and the cell, and can be used to assess the activity of the mitochondrial proton pumps, electrogenic transport systems, and the activation of the mitochondrial permeability transition (Rottenberg and Wu, 1998).

6.2 Mitochondria and cancer

Otto Warburg proposed in 1930 that respiratory deficiency might result in differentiation of cells and hence neoplastic transformation. Early studies of differences between the mitochondria of normal cells and those of cancer cells focused on the respiratory deficiencies common to rapidly growing cancer cells (Modica-Napolitano and Singh, 2002). Mitochondrial alterations have been implicated in a wide variety of acute and chronic human conditions, including cancer, intoxication, neuro-degenerative diseases, and aging (Horbinski and Chu, 2005). While precise contribution of mitochondria to carcinogenesis remains unclear, it has been reported that mitochondrial DNA (mtDNA) mutations, ranging from a single base mutation to a large deletion, were detected in a variety of tumours (Dias and Bailly, 2005). The analysis of the complete mitochondrial genome of 10 colorectal cancer cell-lines has shown that seven displayed mtDNA point-mutations that were not detected in normal tissue from which the tumour is derived (somatic mutation). To date, no particular mtDNA mutations have been correlated to a specific cancer.

6.3 Mitochondria as cancer drug targets

Mitochondria play a key role in the regulation of apoptosis and recent findings suggest that many apoptotic pathways converge at a single event- mitochondrial membrane permeabilisation (Barnard *et al.,* 2003). Targeting mitochondria has the potential to overcome the two overriding problems in cancer chemotherapy- the common occurrence of drug-resistant tumour cells and the lack of selectivity of cancer drugs in differentiating between tumour cells and normal tissues (Barnard *et al.,* 2004).

Compounds that specifically target cancer cell mitochondria must have a function that is based on differences in the bioenergetic or protein composition of the transformed cells (Don and Hogg, 2004). It is well established that transformed cells take up glucose more rapidly than normal counterparts and derive a larger proportion of their energy through aerobic glycolysis. Significantly, carcinoma cells have elevated plasma and mitochondrial membrane potentials relative to normal cells, leading to a more rapid accumulation of lipophilic cations, which are concentrated within mitochondria in response to the negative mitochondrial membrane potential (Barnard *et al.,* 2004).

Lonidamine is an anti-cancer agent that has been used in combination chemotherapy and has undergone clinical trials for the treatment of tumours that are refractory to conventional chemotherapy (Don and Hogg, 2004). Evidence indicates that it inhibits aerobic glucose utilisation, a mechanism that is probably mediated through a direct inhibition of mitochondrial-associated hexokinase. Increased expression and activity of hexokinase, which is associated with the outer mitochondrial membrane, is a feature of cancer cells that enables them to maintain high rates of glucose use. A good summary of drugs that target mitochondrial functions to control tumour growth has recently appeared in the literature (Dias and Bailly, 2005).

6.3.1 Lipophilic cations as potential chemotherapeutic agents

A variety of lipophilic cations with delocalised charges accumulate in the mitochondria of carcinoma-derived cells more rapidly than in most untransformed cells (Rideout *et al.,* 1989). These compounds concentrate in mitochondria due to their lipophilic-cationic character and exhibit preferential cytotoxicity to carcinoma cells with hyperpolarised membranes (Summerhayes *et al.,* 1982; Davis *et al.,* 1985; Nadakavukaren *et al.,* 1985; Chen, 1988). A study aimed at determining the mechanism of action of cationic phosphonium salts against carcinomas, with particular emphasis on the effects of tetraphenyl phosphonium chloride (TPP) on FaDu human hypopharyngeal squamous carcinoma cells was carried out (Rideout *et al.,* 1994). The abnormally high mitochondrial membrane potential in FaDu cells

caused preferential concentration of TPP in mitochondria, leading in turn to mitochondrial membrane damage.

Several structurally diverse lipophilic cations have demonstrated strong activity by concentrating in mitochondria, for example, rhodamin 123 (Johnson *et al.,* 1980), dequalinium (Weiss *et al.,* 1987), pyronine Y (Darzynkiewizc *et al.,* 1986), ditercalinium (Roques *et al.,* 1979), AA-1 (Sun *et al.,* 1994) and MKT-077 (Koya *et al.,* 1996), the latter having advanced to Phase **I** clinical trial. It has been shown that the mitochondria of carcinoma cells derived from kidney, ovary, pancreas, lung, adrenal cortex, skin, breast, prostate, cervix, vulva, colon, liver and testis accumulated Rh123 (*Fig 6.2*) to a greater extent and with a longer retention time than normal cells derived from bladder, breast, kidney, oesophagus, skin and lung (Don and Hogg, 2004).

Dequalinium chloride (DEQ) (*Fig 6.2*) has been shown to prolong the life span of mice implanted with bladder carcinoma >190%, which was significantly greater than other anti-cancer drugs that were tested (i.e., cisplatin, cytosine arabinoside, methotrexate and cyclophosphamide) (Berlin *et al.,* 1998). DEQ was shown to induce a delayed inhibition of cell growth in cultured human carcinoma cells as well as cause a selective loss of mitochondria DNA (mtDNA).

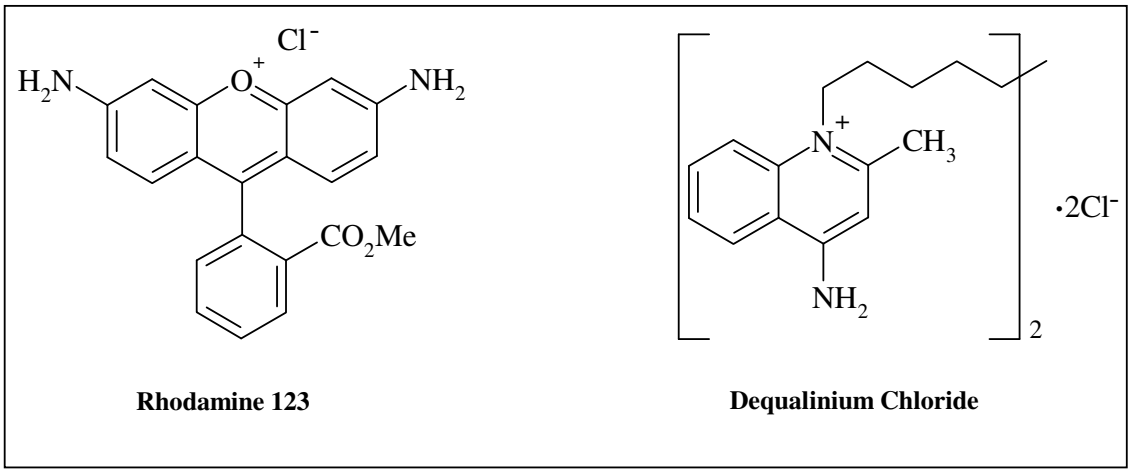

Fig 6.2: Some examples of lipophilic cations that have been shown to concentrate in mitochondria.

After screening more than 1000 lipophilic cations, Chen and co-workers found that the monovalent lipophilic cation, 2,6-bis-(4-amino-phenyl)-4-[4-

(dimethylamino)phenyl]thiopyrylium chloride (AA1) (*Fig 6.3*), displayed remarkable anti-carcinoma activity both *in vitro* and *in vivo (Sun et al., 1994)*. Compared with previously reported anti-carcinoma lipophilic cations such as rhodamine 123 and dequalinium chloride, AA1 appeared to display a more effective anti-carcinoma activity *in vivo*.

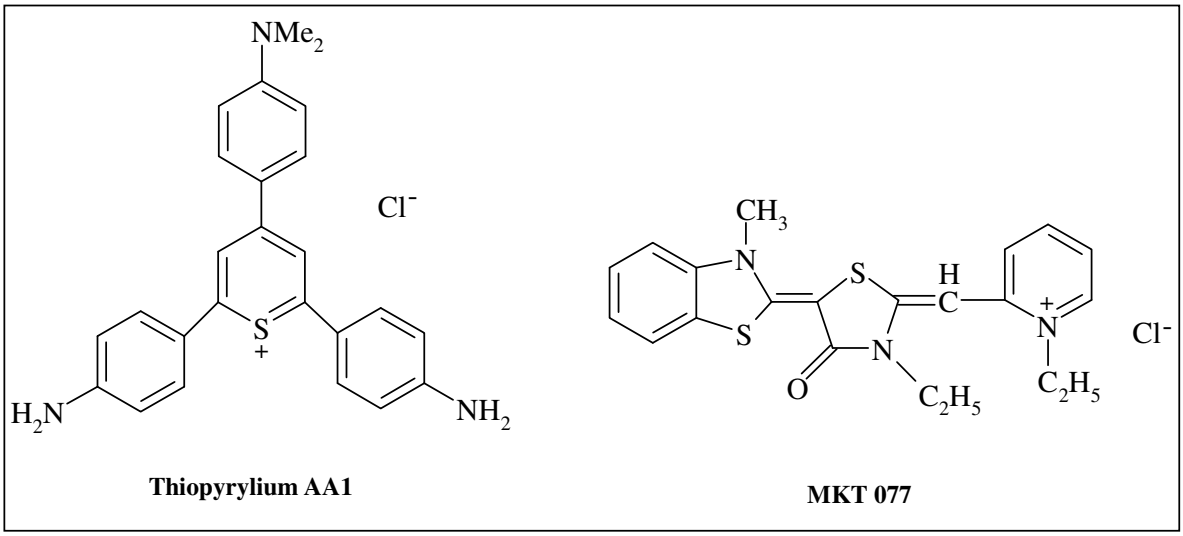

Fig 6.3: Some examples of lipophilic cations that have been shown to concentrate in mitochondria.

Rhodacyanine MKT-077 (*Fig 6.3*) accumulates in tumour cell mitochondria leading to ultrastructural changes, loss of mitochondrial DNA, generalised perturbation of mitochondrial membrane and non-specific damage to membrane enzymes (Sun *et al.,* 1994). It has been shown to possess significant activity against human renal carcinoma, prostate carcinoma, and melanoma tumours implanted in nude mice (Berlin *et al.,* 1998). Since many normal cells are reliant on oxygen consumption and oxidative phosphorylation for ATP production and tumours are primarily reliant on glycolysis for production of ATP, anti-mitochondrial agents that target oxidative phosphorylation pathways are likely to be limited in their therapeutic application by host toxicity and poor anti-tumour selectivity (McKeage *et al.,* 2002).

Interestingly, one research group manipulated membrane potentials in order to determine the uptake of TPP on FaDu (Rideout *et al.,* 1994). They found that depolarisation of the plasma membrane caused a 4-fold decrease in uptake of TPP and depolarisation of both plasma and mitochondrial membranes caused a 16.3-fold decrease in uptake. It is of further interest to note that, although

increased membrane potential is necessary to achieve selective cytotoxicity by delocalised lipophilic cations, it is not sufficient on its own (Modica-Napolitano and Singh, 2002). If this were the case, then cardiac muscle cells, which have been shown to exhibit high mitochondrial membrane potential would be susceptible to the cytotoxic effects of these compounds (i.e. MKT077 or dequalinium). Conversely, myelotoxicity is less of a problem with these compounds than conventional chemotherapeutics, because bone marrow cells have a low $\Delta\Psi_m$ (Don and Hogg, 2004).

6.4 Analysis of mitochondrial membrane potential

6.4.1 Fluorescent probes

Probes include those which exhibit optical and fluorescence activity after accumulation into energised systems (Cossarizza and Salvioli, 1997). Examples are 3,3'-diehexiloxadicarbocyanine iodide [$DiOC_6$ (3)], nonylacridine orange (NAO), safranine O and rhodamine-123 (Rh 123), radiolabelled probes, (i.e., [^{3}H]methyltriphenyl-phosphonium) and unlabelled probes used with specific electrodes [i.e., tetraphenyl-phosphonium ion (TPP+)]. These probes allow the analysis of changes in mitochondrial membrane potential (rhodamine 123) or modifications of mitochondrial mass (nonyl acridine orange) (Cossarizza *et al.,* 1993). However, the results these probes can put in evidence are expressed as decreases or increases in fluorescence intensity, so that variations of membrane potential are usually expressed as decreases or increases in this fluorescent intensity. For example, while rhodamine 123 is highly specific for living cells, it does not possess the ability to differentiate between mitochondria of low and high membrane potential (Gravance *et al.,* 1999).

While fluorescent labelling of cells provides important information regarding the functional status of the cell, the true utility of fluorescent markers is the ability to assess these staining patterns using flow cytometry (Gravance *et al.,* 1999). Flow cytometry (FCM) allows the characterisation and analysis of several cell parameters and functions, such as lymphocyte phenotype cell cycle, apoptosis, among others (Cossarizza *et al.,* 1993). A consistent advantage of FCM techniques is the possibility to analyse thousands of living cells in a few seconds.

The lipophilic cationic compound 5,5',6,6'-tetrachloro 1,1',3,3'-tetra ethylbenzimidazolyl carbocyanine iodide (JC-1) possesses the unique ability to differentially label mitochondria with high and low membrane potential (Gravance *et al.,* 2001). JC-1 is more advantageous over rhodamines and other carbocyanines capable of entering selectively into mitochondria, since it changes reversibly its colour from green to orange as membrane potentials increase (over values of about 80-100 mV) (Cossarizza and Salvioli, 1997). This property is due to the reversible formation of JC-1 aggregates upon membrane polarisation that causes shifts in emitted light from 530 nm (*i.e.*, emission of JC-1 monomeric form) to 590 nm (*i.e.*, emission of J-aggregate) when excited at 490 nm; the colour of the dye changes reversibly from green to greenish orange as the mitochondrial membrane becomes more polarised.

Both colours can be detected using the filters commonly mounted in all flow cytometers, so that green emission can be analysed in fluorescence channel 1 (FL1) and greenish orange emission in channel 2 (FL2) (Cossarizza and Salvioli, 1997). The main advantage of using JC-1 is that it can be both qualitative, considering the shift from green to orange fluorescence emission, and quantitative, considering the pure fluorescence intensity, which can be detected in both FL1 and FL2 channels. This cytofluorimetric method (Salvioli *et al.,* 1997):

- allows the identification of populations with different mitochondria content;
- has already been utilised for studying behaviour of these organelles in a variety of conditions, including apoptosis;
- has been further validated by analysing $\Delta\psi$ at the level of single mitochondria

6.5 Objective of this experiment

The intention of the experiments described below was to determine whether the observed cytotoxicity (*Chapter 5*) was due to loss of mitochondrial membrane potential to either resting lymphocytes or Jurkat cells. Jurkat cells were selected for these experiments as they could be compared to lymphocytes (normal cells).

The expected outcome was that these cationic compounds would selectively accumulate in the mitochondria of Jurkat cells rather than in lymphocytes. Depolarisation of the membrane potential would then lead to a decrease in J-aggregates (orange fluorescence) and an increase in j-monomers (green fluorescence).

The procedure used to analyse mitochondrial membrane potential changes was adapted from the literature (Cossarizza and Salvioli, 1997). Valinomycin, a classical K+ ionophore that dissipates the membrane potential but not the pH gradient, was used to reduce the orange fluorescence emission of JC-1 (Cossarizza *et al.,* 1993).

6.6 Materials and methods

6.6.1 Reagents

- Cell culture medium (RPMI + 10% FCS).
- Phosphate buffered saline (PBS).
- JC-1 (Sigma-Aldrich).
- Valinomycin (Sigma-Aldrich).
- [4]**Pg 8** (0.711 µM and 1.422 µM) and **[Au(dppe)$_2$]Cl** (0.131 µM and 0.262 µM) –Jurkat.
- **Pg 8** (100 µM and 200 µM) and **[Au(dppe)$_2$]Cl** (0.903 µM and 1.806 µM)-lymphocytes.

6.6.2. Cell cultures

Human T-cell line (Jurkat) was cultured in RPMI 1640 supplemented with 10% v/v heat-inactivated FCS and 1% penicillin-streptomycin. Cells were maintained in a humidified atmosphere of 5% carbon dioxide at 37 ℃.

[4] The concentrations used here represent the IC_{50} values (and double) that were obtained in cytotoxicity assays (Chapter 5).

6.6.3. Flow cytometric analysis of mitochondrial membrane potential changes

Cells (Jurkat = 3 x 10^5 or lymphocytes = 2 x 10^6 cells/ml) were treated with $[Au(dppe)_2]Cl$ and **Pg 8** for 24 h [10 mins with 10 µM valinomycin]. After incubation, all the untreated and treated cells were decanted from the flasks into centrifuge tubes and centrifuged for 5 min at 500 g. The cell pellets were suspended in 1 ml of complete RPMI followed by addition of 100 µl of 1.5 µg/ml JC-1. The suspension was mixed well and samples kept in the dark for 15-20 minutes. At the end of incubation period, the cells were washed twice while centrifuging at 500 g (5 min) with double volume of cold PBS. The pellet was then re-suspended in 1 ml of PBS (10% FCS).

Analyses were performed using a flow cytometer (Beckman Cytomics FC 500) equipped with a single 488 nm argon laser. The instrument was programmed to calculate the ratio of FL2:FL1, which would signify either hyperpolarisation or depolarisation of the mitochondrial membrane. An increase in the ratio would indicate hyperpolarisation (less j-monomers and more j-aggregates) while a decrease would signify depolarisation due to reduction of orange fluorescence (more j-monomers and less j-aggregates).

6.6.4. Statistical methods

Statistical analyses were performed by One Way Analysis of Variance (ANOVA) followed by Dunnett's Multiple Comparison Test to determine the treatments that were significantly different from the fresh, viable cells. The averages (± SEM) for each treatment represent at least six independent experiments. However, Student's t-test was performed for section 6.7.2. The treatment that was significantly different from the untreated cells is denoted with an asterix (*) and $P<0.05$ was considered significant.

6.7 Results and discussion

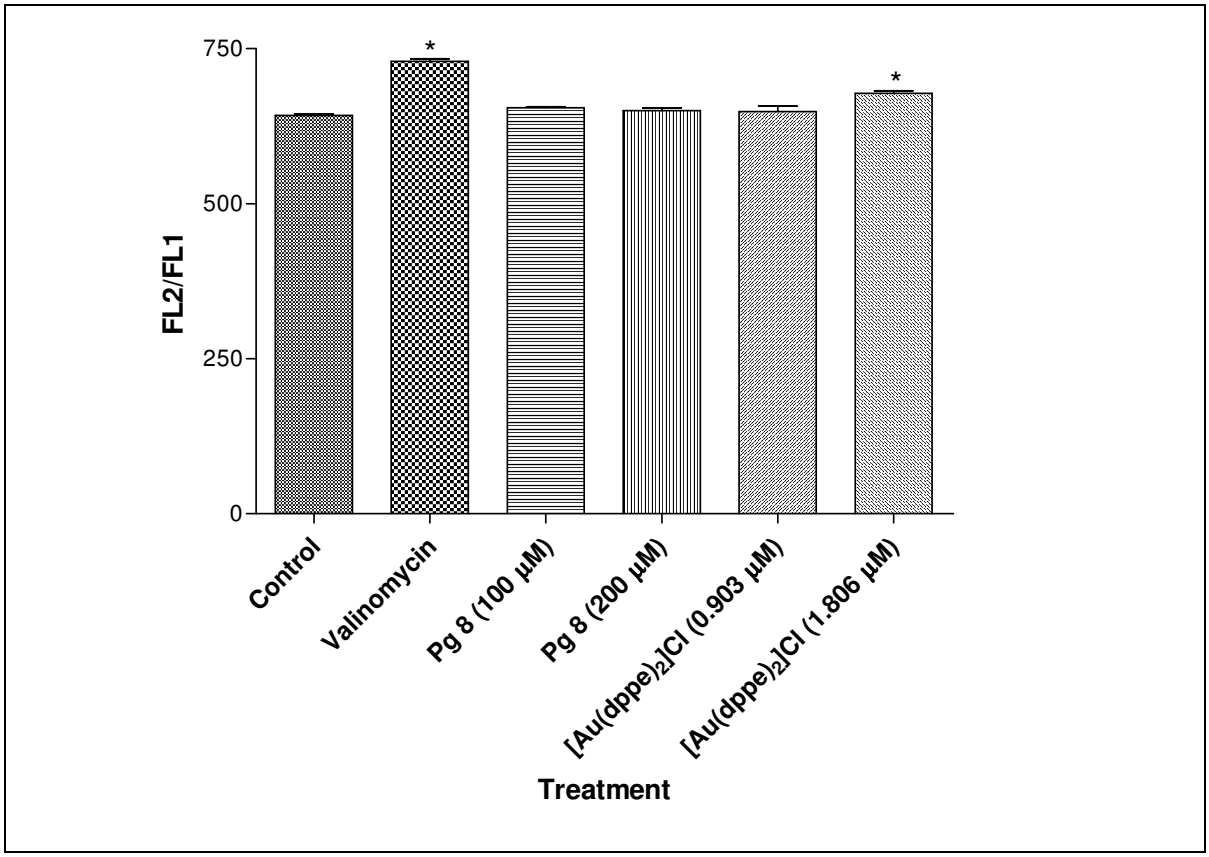

Fig 6.4: Ratio of J-aggregates (FL2): J-monomers (FL1) in resting lymphocytes after treatment (24 h) with valinomycin (10 µM), **Pg 8** (100 µM and 200 µM) and **[Au(dppe)$_2$]Cl** (0.903 µM and 1.806 µM). The cells were stained with JC-1 for 30 mins and analysed by flow cytometry. The data shown here is an average of at least 6 independent experiments.

Exposure of valinomycin (10 µM) and [Au(dppe)$_2$]Cl (1.806 µM) to resting lymphocytes led to an increase in ratio between the j-monomers and j-aggregates (ratio of FL2:FL1 increased) (*Fig. 6.4*). This indicated that polarisation of the membrane potential had taken place as the amount of JC-1 aggregates were found to be significantly higher (P<0.01) than those found in untreated cells. Cells treated with **Pg 8** (100 and 200 µM) and [Au(dppe)$_2$]Cl (0.903 µM) did not induce any loss of mitochondrial membrane potential.

Hyperpolarisation of the mitochondria of lymphocytes has been described by authors and it seems to represent a pre-requisite for rapid mitochondrial-mediated apoptotic cell death that eventually leads to the loss of mitochondrial membrane potential (Giovannini *et al.,* 2002). These hyperpolarisation effects can result from

different actions, such as increased mitochondrial mass and number per cell or an increase in matrix volume, the latter leading to swelling and rupture of the outer membrane, followed by a decrease in $\Delta\Psi_m$. Another research group has shown that methyl protodioscin, a furostanol bisglycoside with anti-tumour properties induced hyperpolarisation in mitochondria of human chronic myelogenous leukaemia K562 cells, with the loss of mitochondrial membrane permeabilisation as a secondary response (Liu *et al.,* 2005).

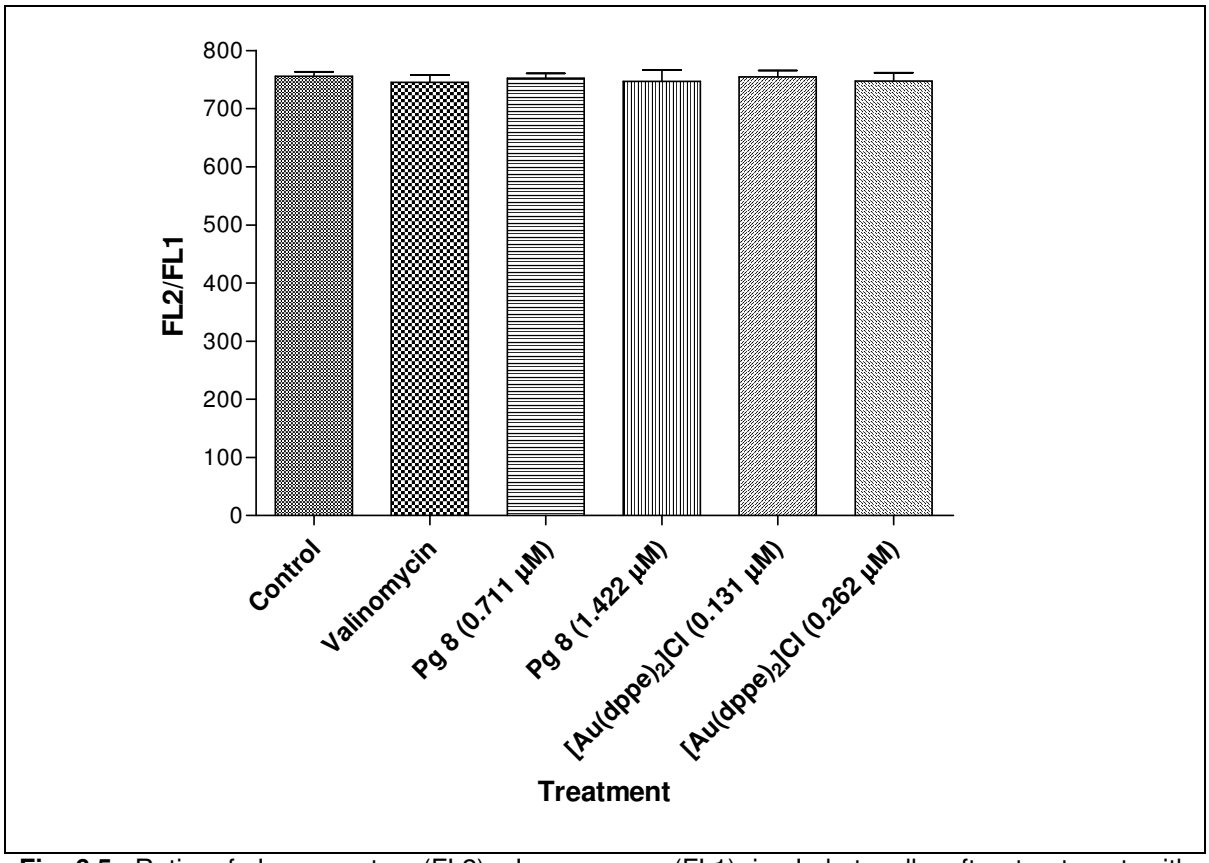

Fig 6.5: Ratio of J-aggregates (FL2): J-monomers (FL1) in Jurkat cells after treatment with valinomycin (10 µM), **Pg 8** (0.711 µM and 1.422 µM) and **[Au(dppe)$_2$]Cl** (0.131 µM and 0.262 µM). The cells were stained with JC-1 for 30 mins and analysed by flow cytometry. The data shown here is an average of at least 6 independent experiments.

No changes in membrane potential of Jurkat cells occurred when exposed to the test compounds (*Fig 6.5*). The expectation was that the compounds would accumulate in the mitochondria of cancerous cells faster and induce depolarisation of the mitochondrial membrane. It is worth noting that untreated Jurkat cells (Mean FL2:FL1 ratio = 756) were more polarised (P<0.0001) than untreated resting lymphocytes (Mean FL2:FL1 ratio = 642) .

From the above results, it is clear that the experimental compounds did not depolarise the mitochondrial membrane of Jurkat cells at low concentrations as well as after 24 hours. Hence, two further experiments were designed to determine whether longer incubation times or higher drug concentrations would lead to changes in membrane potentials.

6.7.1 Determination of mitochondrial membrane potential changes of cells exposed to higher drug concentrations

To determine whether $[Au(dppe)_2]Cl$ induced cytotoxicity was related to changes in the mitochondria, studies of induced toxicity and biochemical alterations in intact rat hepatocytes were carried out (McKeage *et al.,* 2002). Within 30 min of exposure, $[Au(dppe)_2]Cl$ (5-20 µM) had been taken up by isolated hepatocytes and distributed to mitochondria. Within the same period of time, isolated rat hepatocytes formed blebs on the plasma membrane, lost ATP, showed increased oxygen consumption and developed morphological changes in mitochondria as detected by electron microscopy. It also induced rapid dissipation of the inner mitochondrial membrane potential, efflux of calcium, increased mitochondrial respiration, mitochondrial swelling and increased permeability of the inner membrane to cations and protons.

This assay aimed at determining whether the experimental compounds induced a loss of mitochondrial membrane potential at higher concentrations (10 and 15 µM).

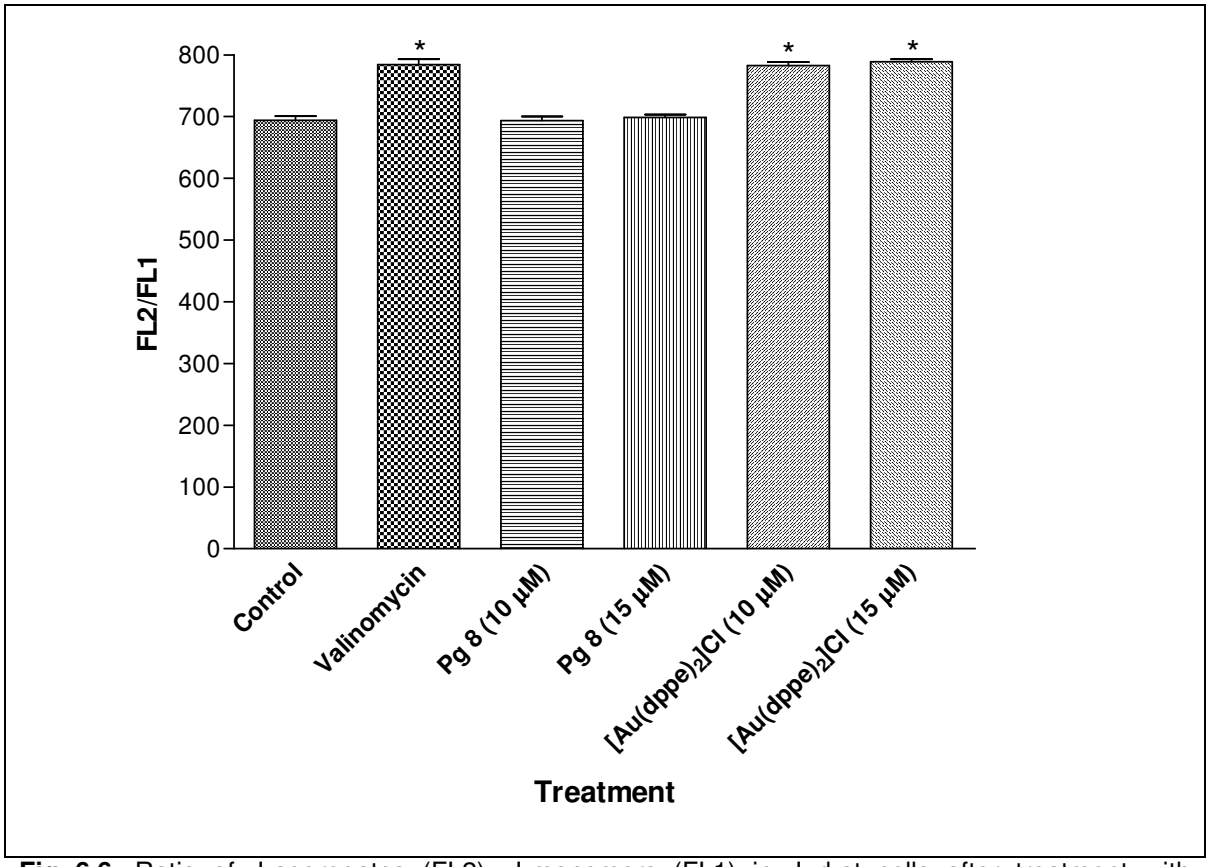

Fig 6.6: Ratio of J-aggregates (FL2): J-monomers (FL1) in Jurkat cells after treatment with valinomycin (10 µM), **Pg 8** (10 µM and 15 µM) and **[Au(dppe)$_2$]Cl** (10 µM and 15 µM). The cells were stained with JC-1 for 30 mins and analysed by flow cytometry. The data shown here is an average of at least 3 independent experiments.

Pg 8 (10 and 15 µM) did not decrease nor increase membrane potentials of Jurkat cells (*Fig 6.6*). There was a significant increase (P<0.0001) in FL2/FL1 ratio of cells that were treated with valinomycin and [Au(dppe)$_2$]Cl. These results also show that [Au(dppe)$_2$]Cl caused changes in the mitochodrial membrane potential of Jurkat cells at concentrations that were much higher (~75 times) than that required to cause death to the cells. Studies carried out with [Au(dppe)$_2$]Cl on isolated heart or hepatocyte mitochondria showed that the rate and degree of drug-induced dissipation of the electrochemical potential difference was concentration dependent (Hoke *et al.,* 1989). At a concentration of 15 and 20 μM [Au(dppe)$_2$]Cl, the dissipation of the electrochemical gradient was not complete. However, exposure of the mitochondria to 30 or 60-µM drug resulted in a complete dissipation of electrochemical gradient.

6.7.2 Determination of mitochondrial membrane potential changes of cells exposed to Pg 8 for 7 days

This experiment involved the incubation of Jurkat cells with **Pg 8** (0.711 µM) for 7 days. The mitochondrial membrane potential changes were monitored every 24 hours to determine the time required for the test compound to induce changes in the mitochondria. It has been shown that the lipophilic cation Rh123 requires at least 6 days to exhibit significant activity against some carcinoma cells (Rideout *et al.,* 1994). It was also shown that TPP caused damage to the mitochondrial inner membrane of FaDu cells under conditions that inhibit cell proliferation by 50% (0.45 µM, 6 day exposure).

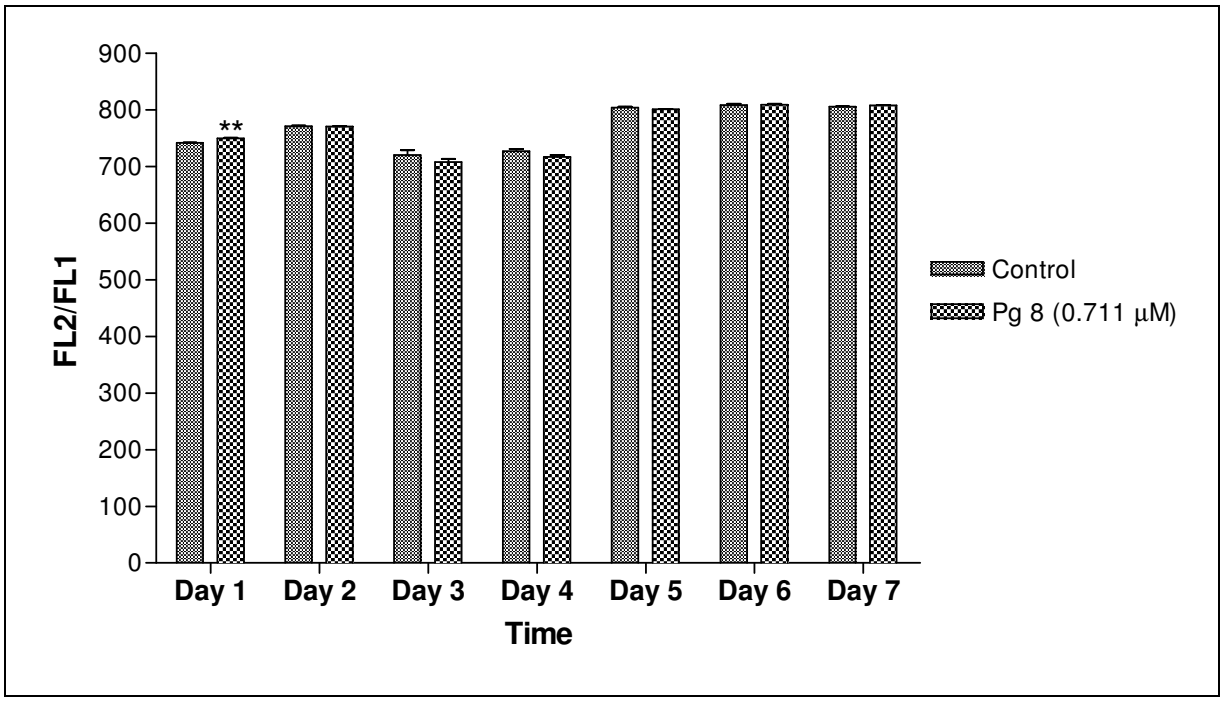

Fig 6.7: Ratio of J-aggregates (FL2): J-monomers (FL1) in Jurkat cells after treatment (7 days) with **Pg 8** (0.711 µM). The cells were incubated in cell culture flasks and samples were analysed by flow cytometry every 24 h. The data shown here is an average of at least 3 independent experiments carried out in triplicate.

The ratio of j-aggregates vs j-monomers on day 1 was higher ($P<0.05$) in Jurkat cells treated with **Pg 8** (0.711 µM) than in untreated cells (*Fig 6.7*). No differences in membrane potentials were noted for the remainder of the study.

6.8 Plasma membrane Potential

The plasma membrane is a lipid bilayer that accommodates a significant number of proteins with diverse structures and tasks necessary for the proper function of the cells (Vámosi *et al.,* 2006). A primary function of the plasma membrane is the maintenance of a potential difference by its ability to barricade the free passage of ions across the membrane (Mann and Cidlowski, 2001). Normally, most cells maintain an electrical potential across the plasma membrane of -60 mV to -70 mV that renders the inside of the membrane more negative than the outside. In living cells, mitochondria are surrounded by the plasma membrane whose membrane potential has been shown to have a pre-concentrating effect on the accumulation of lipophilic cations by mitochondria (Smiley *et al.,* 1991).

Plasma membrane potential (E_m) contributes to the driving force of ions like Ca^{2+} across the plasma membrane and is therefore essential for different signal transduction pathways and the regulation of uptake and excretion of the metabolites (Nolte *et al.,* 2004). The intact plasma membrane integrity includes preservation of its basal function, like a barrier for ions and macromolecular structures, and active transport pumps (Vermes *et al.,* 2000). Apoptosis is characterised by maintenance of an intact plasma membrane during a significant part of its time course.

Until recently, the role of plasma membrane potential in apoptosis has been largely ignored; however, studies have suggested that the plasma membrane potential may be compromised during apoptosis of lymphocytes (Mann and Cidlowski, 2001). For example, in Jurkat cells, three different stimuli that differ in their mode of action, anti-Fas antibody, A23187, and thapsigargin, all induced a loss in plasma membrane potential associated with apoptosis. In lymphocyte-apoptosis, actively induced plasma membrane depolarisation has been previously investigated as the maintenance of the E_m is of vital importance for cells (Nolte *et al.,* 2004).

Dexamethasone has been shown to increase $DiBAC_4(3)$ fluorescence in primary isolated thymocytes (Mann and Cidlowski, 2001). This is consistent with the fact that it increases the percentage of cells undergoing apoptosis and percentage of cells with a depolarised plasma membrane. In the same study, when HeLa cells were treated with 100 nm dexamethasone for 6 h, there was no observable difference in $DiBAC_4(3)$ fluorescence between control and treated cells. These results indicated that the ability of glucocorticoids to induce a loss of plasma membrane potential correlates with their ability to induce apoptosis.

6.9 Analysis of plasma membrane changes by flow cytometry

In order to stain mitochondria, any probe has to enter into the cell and reach the organelles (Salvioli *et al.,* 1997). Its cytoplasmic accumulation is a crucial event, because a critical intracellular concentration is required to obtain an adequate fluorescence signal. Bis-(1,3-dibarbituric acid)trimethine ($DIBAC_4$), is an ionic probe whose distribution across the cell membrane depends on membrane potential (Radosevic *et al.,* 1993). Upon depolarisation, when the inside of the cell becomes more positively charged, more dye enters the cell resulting in an increase in cellular fluorescence. Upon hyperpolarisation, the dye is extruded from the cell resulting in a decrease in fluorescence. The analyses described below investigated whether plasma membrane potential changes occurred when Jurkat cells were treated with the test compounds. The procedure was modified from published methods (Mann and Cidlowski, 2001, Radosevic *et al.,* 1993).

6.10 Materials and methods

6.10.1 Reagents

- Supplemented cell culture medium (RPMI).
- Phosphate buffered saline (PBS).
- $DiBAC_4(3)$ (Sigma-Aldrich)- Stock solution was prepared from ethanol
- Propidium Iodide (PI) (Sigma-Aldrich)
- Dexamethasone (Sigma-Aldrich)

- [5]**Pg 8** (0.711 µM and 1.422 µM) and **[Au(dppe)$_2$]Cl** (0.131 µM and 0.262 µM) –Jurkat
- **Pg 8** (100 µM and 200 µM) and **[Au(dppe)$_2$]Cl** (0.903 µM and 1.806 µM)-lymphocytes

6.10.2 Cell cultures

Human T-cell lines (Jurkat) were cultured in RPMI 1640 supplemented with 10% v/v heat-inactivated FCS and 1% penicillin-streptomycin. Cells were maintained in a humidified atmosphere of 5% carbon dioxide at 37 ℃.

6.10.3 Flow cytometric analysis of plasma membrane potential changes

1.8 ml of cell suspension (Jurkat 3 x 10^5 and lymphocytes 2 x 10^6 cells/ml) was incubated with 0.2 ml of test compounds for 24 hrs at 37°C, 5% CO_2. Dexamethasone (100 nm, 6 hours incubation) was used as a positive control. After incubation period, cells were centrifuged at 500 g for 5 min followed by re-suspension of the pellet in 2 ml of cold complete medium. Centrifugation was carried out and the pellet re-suspended in 900 µl of cold complete medium. 100 µl of $DiBAC_4(3)$ (150 nm) was added to each tube. The cell suspension was incubated for 30 min at 37 ℃, 5% CO_2.

To exclude cells that had lost membrane integrity, 100 µl of propidium iodide (final concentration of 10 µg/ml) was added to each tube and analysis was carried out immediately using flow cytometer (Beckman Coulter FC 500). Propidium iodide fluorescence was measured on FL-3 (650 nm) to exclude non-viable cells. To determine membrane potential, the $DIBAC_4(3)$ fluorescence of 15,000 viable cells was measured on FL-1 (excitation at 488 nm, emission at 530 nm). The percentage of cells with increased $DIBAC_4(3)$ fluorescence was determined by gating on the fresh, viable population of cells.

[5] The concentrations used here represent the IC_{50} values (and double) that were obtained in cytotoxicity assays (Chapter 5).

6.10.4. Statistical methods

Statistical analyses were performed by One Way Analysis of Variance (ANOVA) followed by Dunnett's Multiple Comparison Test to determine the treatments that were significantly different from the fresh, viable cells. The averages ± SEM for each treatment represent at least six independent experiments. However, Student's t-test was performed for the 7-day study. The treatment that was significantly different from the untreated cells is denoted with an asterix (*) and $P<0.05$ was considered significant.

6.11 Results and discussion

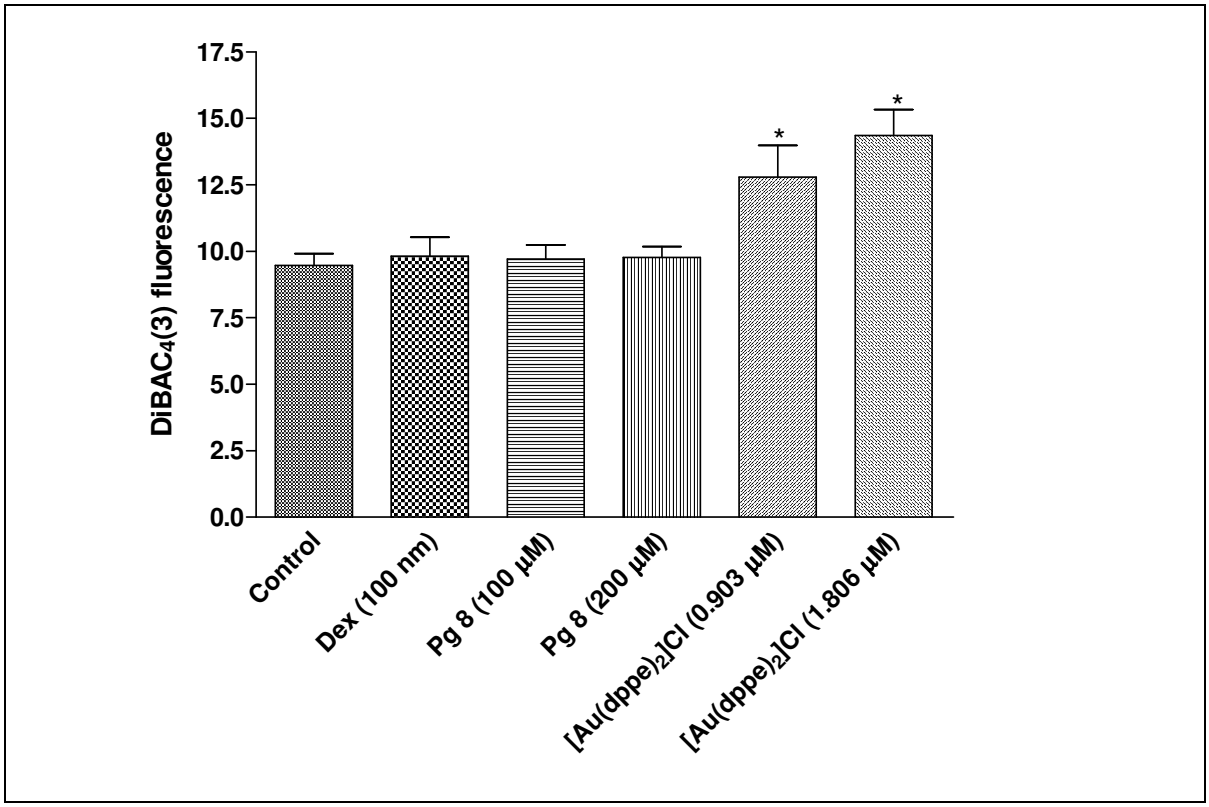

Fig 6.8: Fluorescent intensity of untreated and treated resting lymphocytes. The cells were exposed to the experimental compounds for 24 h followed by incubation with $DIBAC_4(3)$ for 30 min and analysed by flow cytometry. The data shown here is an average of at least 6 independent experiments.

Treatment of lymphocytes with dexamethasone and **Pg 8** (100 and 200 µM) did not show any increase in $DiBAC_4(3)$ fluorescence (*Fig 6.8*). The inability of **Pg 8** to depolarise the plasma membrane potential of lymphocytes is in agreement with

its lack of toxicity even at 100 µM (*Chapter 5*). However, lymphocytes treated with $[Au(dppe)_2]Cl$ (0.131 and 0.262 µM) showed a significant increase ($P<0.05$ and $P<0.01$, respectively) in $DiBAC_4(3)$ fluorescence. This indicates a decrease in plasma membrane potential as a result of depolarisation. These results are in agreement with the high toxicity of $[Au(dppe)_2]Cl$ (IC_{50} = 0.131 µM) to resting lymphocytes (*Chapter 5*) and changes observed in mitochondrial membrane potential. In lymphocytes, plasma membrane depolarisation plays a central role in lymphocyte activation (Mann and Cidlowski, 2001). Activation of the T-cells by antigen-dependent or antigen-independent stimuli results in plasma membrane depolarisation, turnover of polyphosphoinositides, and an increase in free intracellular calcium.

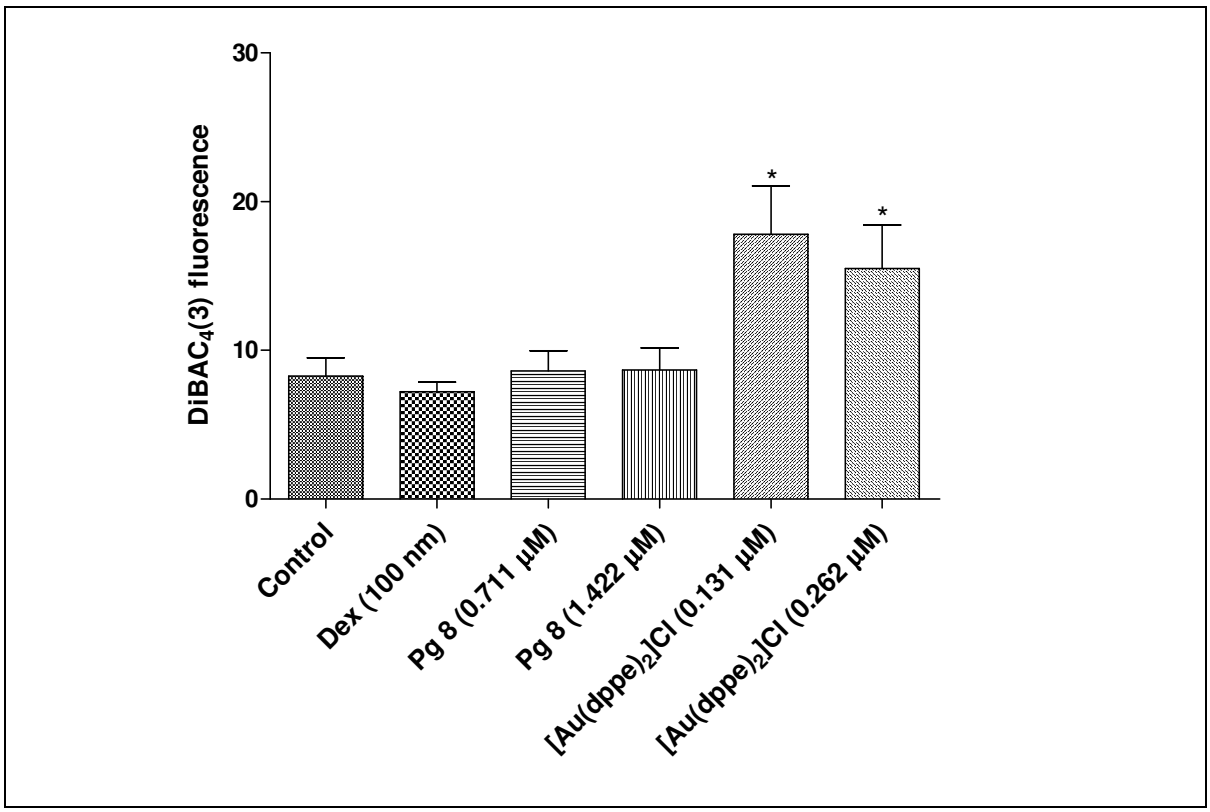

Fig 6.9: Fluorescent intensity of untreated and treated Jurkat cells. The cells were exposed to the experimental compounds for 24 h followed by incubation with $DIBAC_4(3)$ for 30 min and analysed by flow cytometry. The data shown here is an average of at least 6 independent experiments.

Pg 8 and dexamethasone did not induce any plasma membrane potential changes in Jurkat cells (*Fig 6.9*). $[Au(dppe)_2]Cl$ (0.131 and 0.262 µM) caused a significant increase ($P<0.01$ and $P<0.05$, respectively) in $DiBAC_4(3)$ fluorescence. This is in contrast to the results obtained in the determination of mitochondrial membrane

potential changes where no differences were noted between the untreated and treated Jurkat cells.

As previously done in the determination of mitochondrial membrane potential changes, Jurkat cells were exposed to higher drug concentrations (10 and 15 µM).

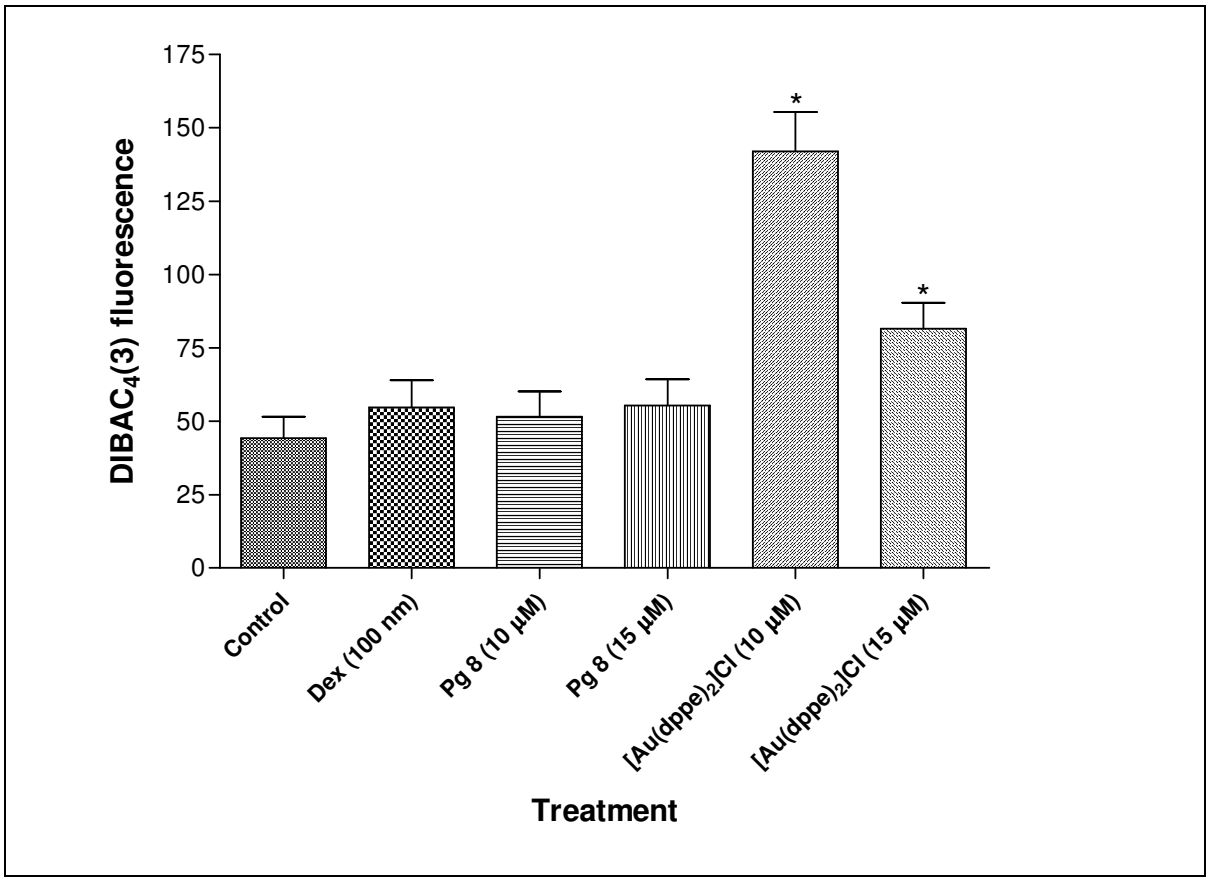

Fig 6.10: Fluorescent intensity of untreated and treated Jurkat cells. The cells were exposed to the experimental compounds (10 and 15 µM) for 24 h followed by incubation with $DIBAC_4(3)$ for 30 min and analysed by flow cytometry. The data shown here is an average of at least 6 independent experiments.

Jurkat cells that were treated with $[Au(dppe)_2]Cl$ (10 and 15 μM) showed a significant increase ($P<0.01$ and $P<0.05$, respectively) in $DiBAC_4(3)$ fluorescence (*Fig. 6.10*). As observed previously, cells treated with Dexamethasone and **Pg 8** caused no loss in plasma membrane potential as the amount of $DiBAC_4(3)$ fluorescence was not significantly higher than that found in the untreated cells.

To establish whether there was any relationship between cytotoxicity of **Pg 8** and plasma membrane potential changes, a time-course experiment was carried out. Jurkat cells were exposed to **Pg 8** (0.711 µM) for 7 days and $DiBAC_4(3)$ fluorescence intensities were monitored every 24 hours.

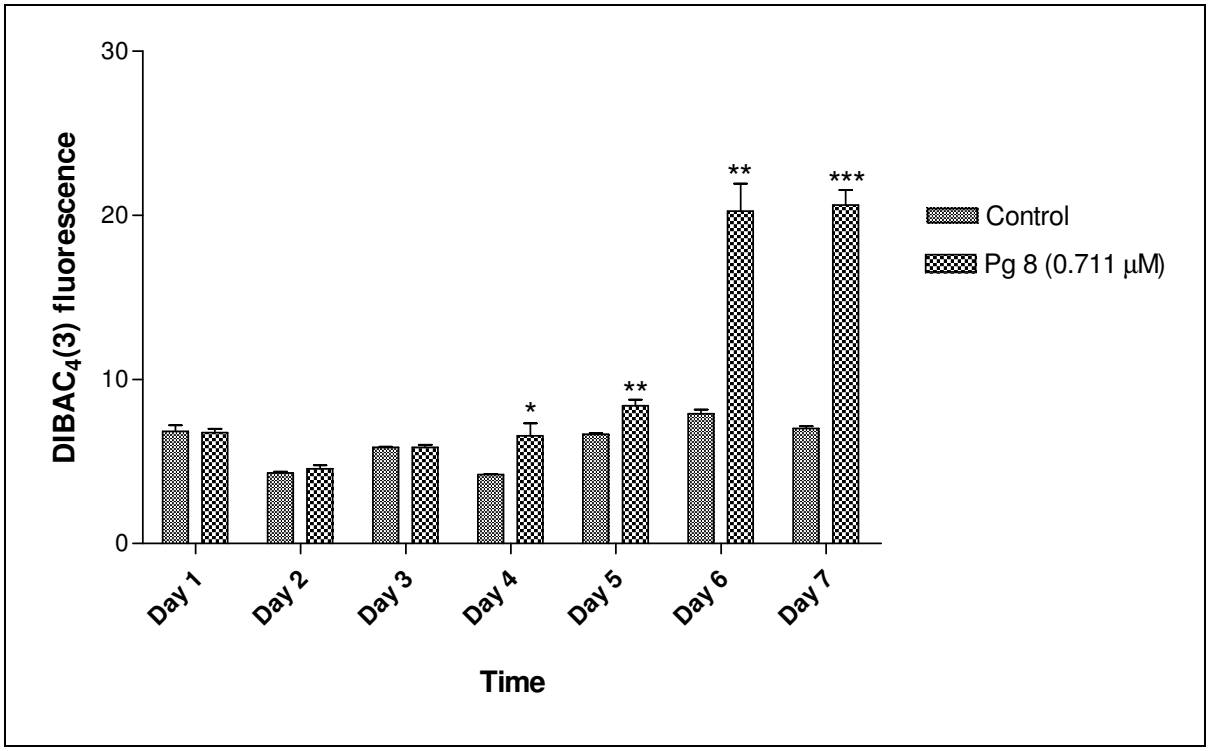

Fig 6.11: Fluorescent intensity of jurkat cells treated with Pg 8 (0.711 µM) for 7 days. The cells were harvested every 24 h, incubated with $DIBAC_4(3)$ for 30 min and analysed by flow cytometry. The experiment was carried out in triplicate.

There was a significant increase ($P<0.05$) in $DIBAC_4(3)$ fluorescence in cells treated with **Pg 8** from day 4 (*Fig.6.11*). This depolarisation of the plasma membrane continued to increase up to day 7 of the experiment. This study showed that **Pg 8** (IC_{50}) depolarised plasma membrane potentials in a time-dependent manner. This is in contrast to the results obtained on mitochondrial membrane potential (*Fig 6.7)*.

6.11.1: Relationship between plasma membrane changes and chemical changes of Pg 8 over a 7 day period

A study was carried out in order to establish a relationship between chemical changes of **Pg 8** and depolarisation of plasma membrane potential over a 7 day period. The stability test was carried out as previously discussed in **Chapter 5** (*5.4.2*). Small amounts of **Pg 8** were dissolved in DMSO, DMSO-d_6 and cell culture medium (EMEM). Two samples were prepared with one containing EMEM with FCS and the other without. The use of cell culture medium with or without FCS was to observe if there were any chemical changes differences between the two samples as a result of presence of thiols in the serum. It has been proposed that the cellular association of auranofin involves ligand exchange with membrane-localised thiols and Et_3PAuCl reacted with whole blood gives P-Au-S species (Berners-Price *et al.,* 1987b).

Both samples were soluble in DMSO (yellow solutions) and no precipitation was observed on addition of EMEM. The two samples were analysed immediately by ^{31}P NMR and every 24 h for six consecutive days (7 days in total) with incubation at 37 ºC between each analysis. Chemical shift changes (ppm) (*Table 6.1*) as well as physical changes were noted. After 24 hours incubation, both solutions changed from yellow to reddish-brown and small amounts of precipitated solids were observed. More precipitation took place on day 2 and day 3. While the sample in EMEM containing 10 % FCS continued to precipitate throughout the duration of the experiment, the one in medium without FCS remained the same from day 3.

Table 6.1. Chemical shift changes (ppm) of $[Pd(d2pyrpe)_2]PF_6]_2$ (**Pg 8**) as monitored by ^{31}P NMR spectroscopy every 24 h for 7 days. Samples were dissolved in DMSO, d_6-DMSO and EMEM with or without Foetal calf serum (FCS). The ratio of the original chemical shift (68.2 ppm) and the new peak (37.6 ppm) is shown in parentheses.

	EMEM without FCS		**EMEM with 10% FCS**	
	Major peak	**Minor peak**	**Major peak**	**Minor peak**
0hr	67.1 (3)	38.5 (1)	68.2	
Day 1	67.2 (1)	38.4 (3)	67.4 (2)	37.5 (1)
Day 2	38.4		67.4 (2)	37.6 (1)
Day 3	38.4		67.4 (2)	37.6 (1)
Day 4	38.6		67.4 (1.5)	37.6 (1)
Day 5	38.4		37.8 (1)	67.4 (0.8)
Day 6	38.5		37.8 (1)	67.3 (0.7)
Day 7	38.5		37.8 (1)	67.3 (1)

Results show that a new phosphorus peak (38.5 ppm) appeared immediately in the sample with EMEM without FCS (*Table 6.1*). The peak of the new species replaced the signal of the original compound (67.2 ppm) by the third day. In contrast, the peak at 37.5 ppm appeared after 24 h in the sample dissolved in EMEM (+10% FCS). From day 1 to day 3, the amount of the original compound was twice the amount of the new species (as indicated by the ratio). On day four, the ratios were reversed and the new species was 1.5 times more than the original compound. The two species reached equilibrium by the seventh day. The major difference was that while the original compound in EMEM (without FCS) was completely replaced by a new species, the one in medium (+10% FCS) seemed to equilibrate with the new species.

The chemical changes observed on day 4 can be correlated with increase in $DIBAC_4(3)$ fluorescence in Jurkat cells treated with **Pg 8**. (*Fig.6.11*). The amount of the new species continued to increase (with subsequent reduction of the amount of the original compound) from day 4 and depolarisation of the plasma membrane continued to increase from day 4 to day 7. It is not clear whether the new species with a chemical shift of 37.6 ppm caused the loss in plasma membrane changes or the presence of both species (67.4 and 37.6 ppm). The

chemical shift 37.6 ppm may be attributed to diphosphine dioxide formed from oxidation of the ligand (d2pyrpe). The ligand in $[Au(dppe)_2]Cl$ (dppe) was shown to form diphosphine dioxide with ^{31}P NMR shift of 38.5 ppm (in methanol) (Berners-Price *et al.,* 1987a). However, the biological properties of some products, e.g. the phosphinites and secondary phosphine oxides, are unknown.

Chapter VII

Apoptosis

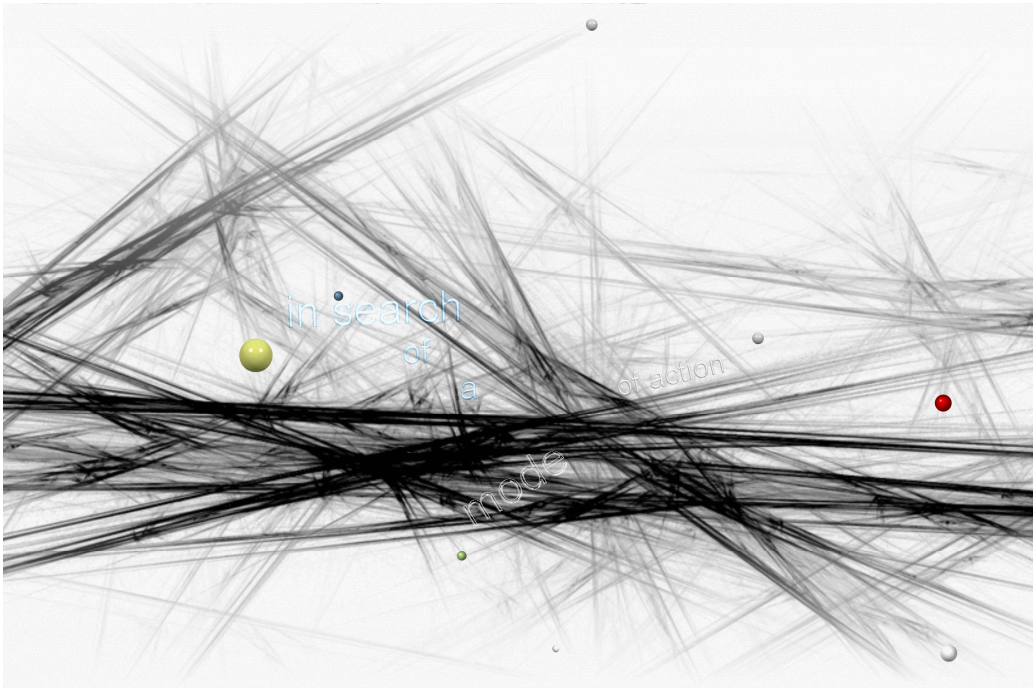

7.1 Introduction

Programmed cell death (PCD), of which apoptosis is the most common morphological expression, is described as an orchestrated collapse of the cell (Ludovico *et al.,* 2002). This process plays an important role in the normal development of the cell and homeostasis of multicellular organisms. Apoptosis serves many critical functions, such as cell deletion during embryonic development, balancing cell numbers in continuously renewing tissues, hormone-dependent involution in the adult, immune system development, selective immune cell deletion, and many other physiologic processes (Allen *et al.,* 1997). Continuous signalling by growth factors, hormones, cytokines, cell-cell contacts and cell-matrix interactions are necessary for cells to refrain from undergoing apoptosis, keeping them alive (Vermes *et al.,* 2000). Cells that are most sensitive for survival signals stay alive and those that cannot compete with their more avid sister cells undergo apoptosis due to relative shortness of survival factors.

7.1.1 Apoptosis vs necrosis

In the middle of the last century, the concept of apoptosis emerged with its unique and dynamic morphological features that are distinguishable from senescence or necrosis, such as cell shrinkage, plasma membrane blebbing, chromatin condensation, nuclear membrane breakdown, and formation of small vesicles from the cell surface known as apoptotic bodies (Jiang and Wang, 2004). After apoptosis, phagocytes rapidly engulf the apoptotic bodies, and thus a potential inflammatory response is avoided. If apoptotic cells are not phagocytosed, they may develop secondary necrosis and cells undergoing post-apoptotic necrosis have been reported to reduce capacity to promote inflammation compared with primary necrotic cells (Magner and Tomasi, 2005).

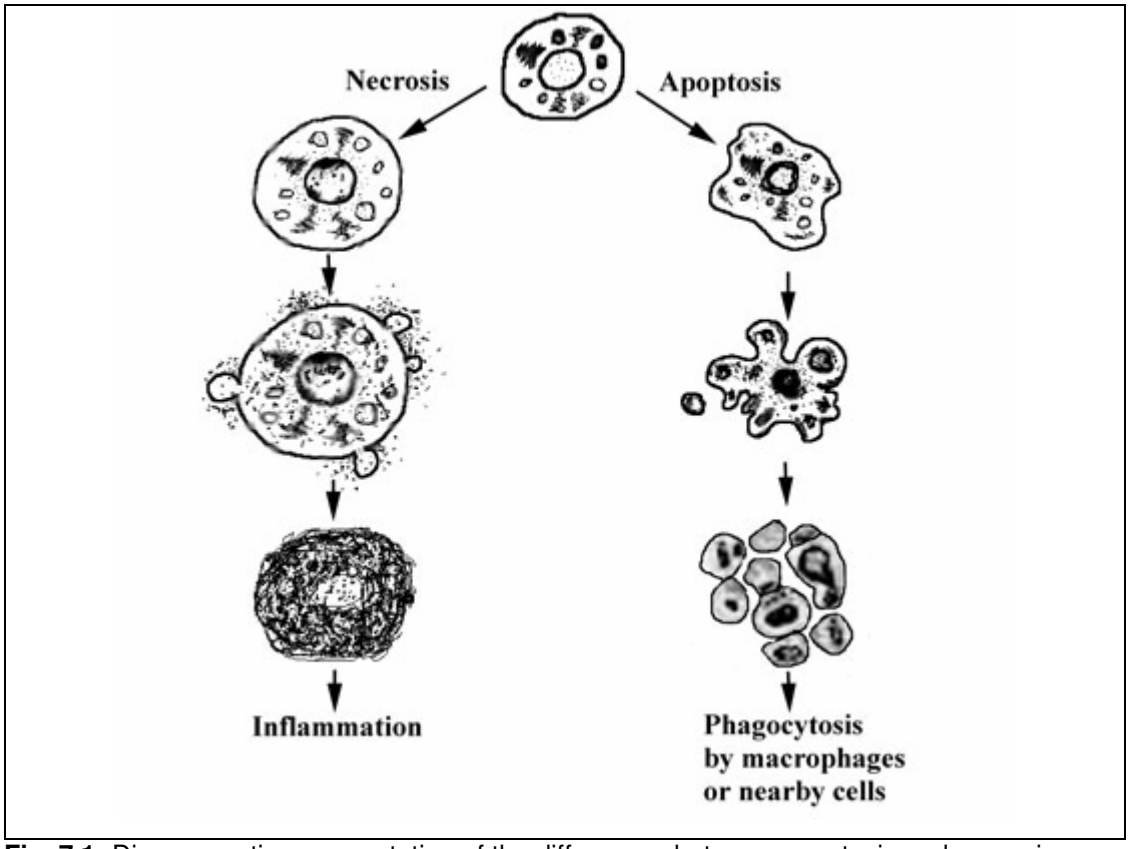

Fig. 7.1: Diagrammatic representation of the differences between apoptosis and necrosis.

Necrosis occurs only in response to a pathologic form of cellular injury and generally affects large groups of cells, characteristically causing an inflammatory response on tissue level (Allen *et al.,* 1997). ATP depletion is a critical precursor to the morphological changes occurring in the necrotic cell. Lethal levels of different toxicants may trigger either apoptotic or necrotic cell death, depending on the cell type and severity of the injury (Orrenius, 2004).

At least two major apoptotic pathways have been described in mammalian cells (Ludovico *et al.,* 2002). One requiring the participation of mitochondria, called "intrinsic pathway," and another in which the mitochondria are bypassed and caspases are activated directly, called "extrinsic pathway".

7.1.2 Apoptosis and mitochondria

Apoptosis induced by extracellular cues and internal insults such as DNA damage is mainly dependent on mitochondria, with the perturbation of inner membrane as an early event (Liu *et al.,* 2005). Mitochondrial membrane permeabilisation

(MMP), regulated by the mitochondrial permeability transition pore (MPT- a voltage dependent, cyclosporine A (CsA) sensitive, high conductance inner membrane channel), is widely accepted as being central to the process of mitochondrially induced apoptosis (Barnard *et al.,* 2004). Extensive evidence indicates that during apoptosis, the outer mitochondrial membrane (OMM) becomes permeable to intermembrane space proteins, including cytochrome *c* (Orrenius, 2004). Once released, cytochrome *c* promotes the activation of pro-caspase-9 directly within the apoptosome complex.

Four major arguments suggest the involvement of mitochondria in apoptosis (Susin *et al.,* 1998):

- Kinetic studies indicate that mitochondria undergo major changes in membrane integrity before classical signs of apoptosis manifest.
- Cell-free systems demonstrate that mitochondrial products are rate limiting for the activation of caspases and endonucleases in cell extracts.
- Pharmacological data indicate that certain drugs that stabilise mitochondrial membranes can prevent apoptosis.
- Extensive analysis of the proto-oncogene product Bcl-2 and its homologs has revealed that they act on mitochondria to regulate apoptosis.

Ever since the discovery that the Bcl-2 protein resides in mitochondrial membranes, the world of mitochondrial physiology and apoptosis has been inextricably linked (Reed *et al.,* 1998). The Bcl-2 family consists of both cell death promoters and cell death preventers. Mammalian species appear to contain at least 14 members, including the anti-apoptotic proteins Bcl-2, Bcl-XL, Mcl-1, A1/Bfl-1, and Bcl-W, and the pro-apoptotic members Bax, Bcl-XS, Bak, Bad, Bik, Bim, Bid, Hrk and Bok. Members of the Bcl-2 family proteins modulate permeabilisation of the OMM (Orrenius, 2004). Bcl-2 and Bcl-XL inhibit protein release whereas Bax and Bak stimulate this release. However, the precise mechanisms whereby mitochondrial proteins cross the OMM during apoptosis, and how Bcl-2 family proteins regulate this process are less certain.

The process of cell death is gene-regulated and elicits degradation of intracellular components and changes of plasma membrane (PM) structure (van Engeland *et al.,* 1996). These alterations of cellular constitution probably serve the purpose of elimination by phagocytosis before the dying cell provokes an inflammatory response. The mechanisms of the breakdown of plasma membrane potential (E_m) and the regulation of ion channels during apoptosis are under debate (Nolte *et al.,* 2004). These processes located at the plasma membrane are of great importance due to their key role in the regulation of apoptotic volume decrease (AVD), a feature that distinguishes apoptosis from necrosis. To date, breakdown in E_m has been described for a few apoptosis inducing agents like inducing Fas-antibodies, Ca^{2+}- ionophores, thapsigargin and dexamethasone.

7.1.3. "Extrinsic pathway"

Apoptosis was recognised as death by orchestrated sequence of countless cuts by hydrolytic enzymes, which degrade macromolecular structures like DNA and cytoskeleton, which underlie the observed apoptotic morphology (Vermes *et al.,* 2000). Members of a family of cysteine proteases play a directing role in this hydrolytic eruption. These proteases called caspases, appear to be the major players involved in the morphological process described in apoptosis, namely the ordered disassembly of the cell. All caspases are present constitutively in precursor forms (30-50 kDa) that must be proteolytically cleaved in order to be activated (Orrenius, 2004). An active caspase can subsequently activate additional pro-caspases, like itself, and/or different pro-caspases.

The caspases implicated in apoptosis can be divided into two functional subgroups based on their known or hypothetical roles in the process: initiator caspase (caspase-2,-8, -9 and -10) and effector caspases (caspase-3, -6 and -7) (Wang *et al.,* 2005). The functions of caspases can be summarised as to:

- arrest the cell cycle and inactivate DNA repair;
- inactivate the inhibitor of apoptosis (XIAP); and
- dismantle the cellular cytoskeleton.

In particular, caspase-9-driven apoptotic machinery seems to mainly involve mitochondrial-associated caspase cascade, while caspase-8-mediated apoptosis appears to be of importance in the receptor-mediated, i.e. Fas-mediated, cell death (Giovannini *et al.,* 2002).

Two proteins have been known to trigger apoptosis when released from mitochondria into the cytosol: cytochrome *c* and apoptosis inducing factor (AIF), a putative protease of 50 kDa (Reed *et al.,* 1998). Cytochrome *c* activates caspases through its effects on a protein called Apaf-1 (apoptosis protease activating factor). Upon binding cytochrome *c*, Apaf-1 binds pro-caspase-9, which eventually results in its proteolytic activation. AIF appears to directly activate certain members of the caspase family, resulting in proteolytic processing of their proproteins and production of the mature enzymes.

7.2 Apoptosis and cancer

Aberrations in cell death signalling (in membrane or cytoplasmic receptors; or alterations in genes that govern apoptosis) are involved in the pathogenesis of congenital malformations and many acquired diseases (Vermes *et al.,* 2000). Numerous pathologically induced conditions such as Alzheimer's, autoimmune disease, cancer, and AIDS, often show varying levels of apoptosis, with greatest significance lying in whether deregulation of apoptosis is a primary event in the pathology and subsequent clinical sequelae (Allen *et al.,* 1997). Defective apoptosis facilitates metastasis, because the cells can ignore restraining signals from neighbours and survive detachment from the extracellular matrix (Ray *et al.,* 2006).

Rapid growth of neoplasias appears to be closely associated with an impairment of the tumour cells to enter apoptosis (van Engeland *et al.,* 1996). Several genes involved in the apoptotic process have been found to be mutated or to be dysregulated at the transcriptional level. For instance, the p53 gene, which is thought to induce apoptosis, is frequently mutated in many tumour types. In contrast, over-expression of the bcl-2 gene, which is believed to protect cells from

apoptosis, is frequently observed in various malignancies. It is over-expressed in the majority of patients with low-grade non-Hodgkin's lymphoma and ~ 50% of high grade cases (Don and Hogg, 2004).

7.3 Apoptosis and chemotherapy

Mitochondria are believed to play a fundamental role in the regulation of programmed cell death and consequently in diseases characterised by abnormal apoptotic responses such as cancer (Barnard *et al.,* 2004). Consequently, there is considerable interest in targeting the mitochondrial cell death pathway in the development of new chemotherapeutic agents (*Fig 7.2*). Early results of clinical trials suggest the feasibility of targeting mitochondrial-based apoptosis regulatory pathways in human cancer therapy without limiting toxicity or significant effects on oxidative phosphorylation pathways (McKeage *et al.,* 2002). Augmerosen (G3139), an antisense 18-base phosphorothioate oligonucleotide complementary to the first 16 codons of Bcl-2 mRNA, hybridises to the target mRNA causing decreases in mRNA and protein levels of Bcl-2 on the membrane of the mitochondria. In clinical trials, augmerosen induced decreased Bcl-2 protein in tumour samples; biologically relevant plasma concentrations and clinical anti-tumour responses. These early experiences provide some support for the principle of targeting mitochondria with therapeutic agents to produce selective toxicity and clinically relevant anti-tumour responses.

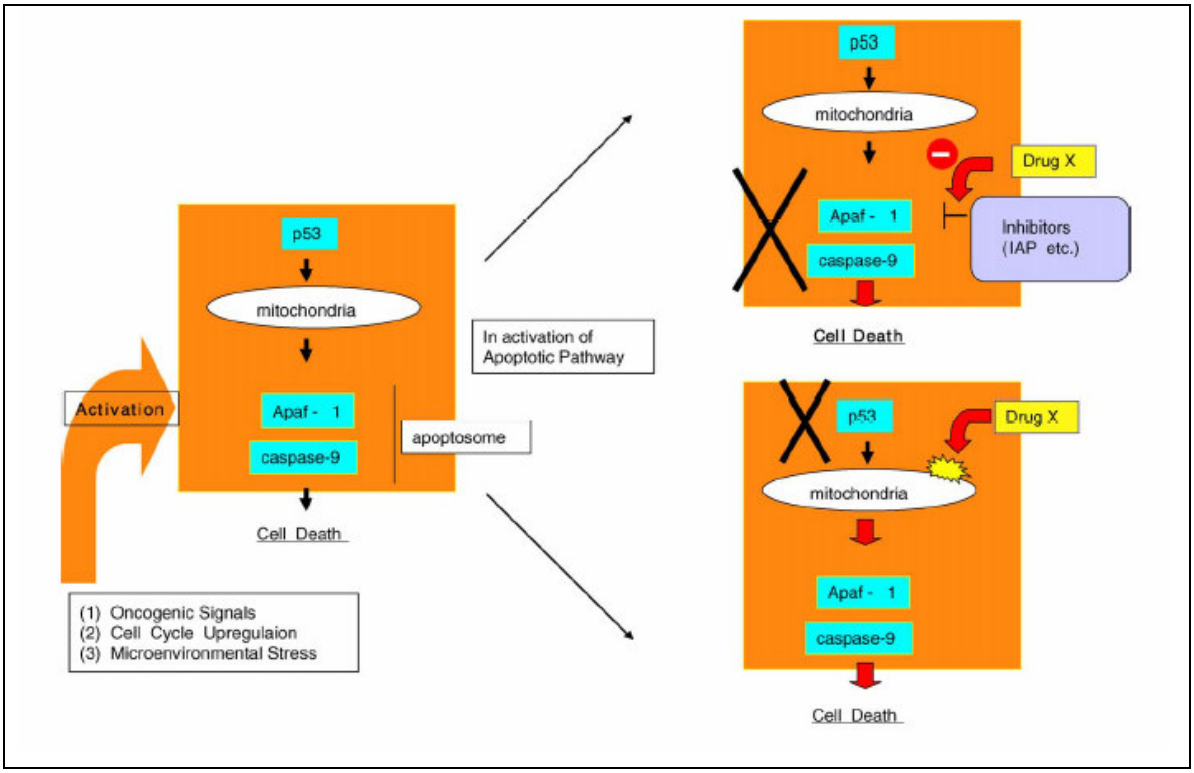

Fig. 7.2: Alteration of the apoptosis pathway in cancer cells and the strategy to induce selective death (Mashima and Tsuruo, 2005).

Induction of apoptosis by targeting specific molecules or pathways is not always straightforward. p53 has long been considered a prime target for therapeutic intervention (Yu, 2006). The role of p53 in apoptosis is complex, as it is able to *promote* and to *suppress* apoptosis. Clinically, the effect of p53 mutations on the sensitivity of tumours to the induction of a chemotherapeutic response has been disputed and so far p53 has failed to demonstrate a definite role in predicting treatment response. Conflicting results have been observed in various cancers. For example, p53 status appears to positively correlate to cisplatin response in ovarian cancer, but it did not seem to play a role in response to chemotherapy in small cell lung cancer (SCLC) patients.

Different cancer cells are likely to have different resistance mechanisms (Makin and Dive, 2001). For example, MCF-7 breast cancer cells are deficient in caspase 3, which renders them insensitive to apoptosis induced by many conventional chemotherapeutic agents. Reconstitution of caspase 3 renders these cells sensitive to etoposide and doxorubicin. Such an approach is, however, unlikely to be helpful in cells that are not deficient in caspase 3. Important emerging

questions are the pattern of alterations in the apoptotic pathway in particular tumours (cell) and the best strategy to exploit them and induce selective tumour cell death (Mashima and Tsuruo, 2005).

7.4 Detection of apoptosis by flow cytometry

In the early stages of apoptosis, changes occur at the cell surface, which until now have remained difficult to recognise (Vermes *et al.,* 1995). One of these plasma membrane alterations is the translocation of phosphatidylserine (PS) from the inner side of the plasma membrane to the outer layer, by which PS becomes exposed at the external surface of the cell. Annexin V is a Ca^{2+} dependent phospholipid-binding protein with high affinity for PS. Hence, this protein can be used as a sensitive probe for PS exposure upon the cell membrane. Translocation of PS to the external cell surface is not unique to apoptosis, but occurs also during cell necrosis. The difference between these two forms of cell death is that during the initial stages of apoptosis the cell membrane remains intact, while at the very moment that necrosis occurs the cell membrane loses its integrity and becomes leaky.

Functional analyses of apoptotic preparations are complicated by the presence of varying proportions of necrotic cells (Magner and Tomasi, 2005). Relying on differences in permeability of plasma membrane of live, dead and apoptotic cells to DNA dyes like propidium iodide (PI), ethidium bromide (EB) and Hoechst-33342 (HO33342), one can discriminate vital, apoptotic and necrotic cells (Vermes *et al.,* 2000). PI is not excluded by necrotic cells and after entering the cell, it intercalates with DNA causing red fluorescence of the necrotic nucleus. Apoptotic cells, which still have an intact membrane exclude PI and are not stained.

Viability tests can also be performed with 7-amino-actinomycin D (7-AAD) which penetrates cell membranes of dying or dead cells and intercalates into double-stranded nucleic acids, especially to guanine cytosine (GC)-rich regions (Huth *et al.,* 2006). 7-AAD can be excited by 488 nm argon laser and emits in the far red range of the spectrum (λ em_{max}: 655 nm) (Derby *et al.,* 2001). Its spectral

emission can be effectively separated from the emissions of phycoerythrin (PE) (λem_{max}: 578 nm). Measurements of annexin V binding, executed simultaneously with the 7-AAD uptake test, provides an excellent way to detect apoptotic cells and to discriminate between different stages of apoptosis at the single cell level. Annexin V assay has been used to measure apoptosis of cell types that occur naturally in suspension (van Engeland *et al.,* 1996). Monitoring apoptosis-related PS exposure by tissue-bound or adherent cell types in cultures faces the problem of PS exposure by sample handling for flow cytometry analysis.

The current study aimed at investigating whether cytotoxicity (*Chapter 5*) was due to induction of apoptosis and/or necrosis by $[Au(dppe)_2]Cl$ and **Pg 8** on Jurkat cells. Annexin V binding assay was carried out and cells were evaluated for apoptosis by flow cytometry. Camptothecin (1 µM), a topoisomerase I inhibitor that efficiently induces apoptosis in Jurkat cells (Sané *et al.,* 2004) was used as a positive control. The procedure was modified from the literature (Allen *et al.,* 1997).

7.5 Materials and methods

7.5.1 Reagents

- RPMI and Foetal Calf Serum.
- Phosphate buffered saline (PBS).
- Binding buffer (238 mg Hepes, 876 mg NaCl, 37.3 mg KCl, 26.5 mg $CaCl_2$, 9.5 mg $MgCl_2$ in de-ionised water, at pH 7.4)
- Annexin V- FITC (BD Biosciences Pharmingen)
- Propidium Iodide (PI) (Sigma-Aldrich)
- Camptothecin (1µM) (Sigma-Aldrich)
- **Pg 8** (0.711 and 1.422 µM)
- $[Au(dppe)_2]Cl$ (0.131 and 0.262 µM)

7.5.2 Cell lines and culture

The human Jurkat cell line was cultured in RPMI 1640 supplemented with 10% v/v heat-inactivated FCS and 1% penicillin-streptomycin. Cells were maintained in a humidified atmosphere of 5% carbon dioxide at 37 °C.

7.5.3 Flow cytometric analysis of apoptosis

Cells (1 x 10^5 cells/ml) were treated with $[Au(dppe)_2]Cl$ and **Pg 8** for 18, 24 and 48 h in cell culture flasks. After an incubation period, cells were decanted from flasks and centrifuged for 5 min at 200 g. The cell pellet was washed with PBS (1% FCS) and resuspended in 1 ml binding buffer. 100 µl of cell suspension was transferred to flow cytometer tubes. 5 µl of Annexin V-FITC and 10 µl propidium iodide were added to some tubes (unstained samples were also prepared). The cell suspensions were mixed gently and incubated for 15 min in the dark at room temperature (25 °C). 400 µl of binding buffer was then added to each tube and analysis was carried out within an hour with a flow cytometer (Beckman Coulter FC 500).

7.5.4 Statistical methods

All assays were performed at least three times and results are presented as ± S.E.M. The statistical evaluation of the results was performed by two way ANOVA followed by Bonferroni's Multiple Comparison Test. Significance was established at $P<0.05$. The treatment that was significantly different from the fresh, viable cells is denoted with an asterix (*).

7.6 Results and discussion

Fig 7.3 shows the percentages of cells undergoing various stages of apoptosis and are an average of three separate experiments (±S.E.M). Figure 7.4 shows actual histograms of treated and untreated cells undergoing apoptosis (48 h).

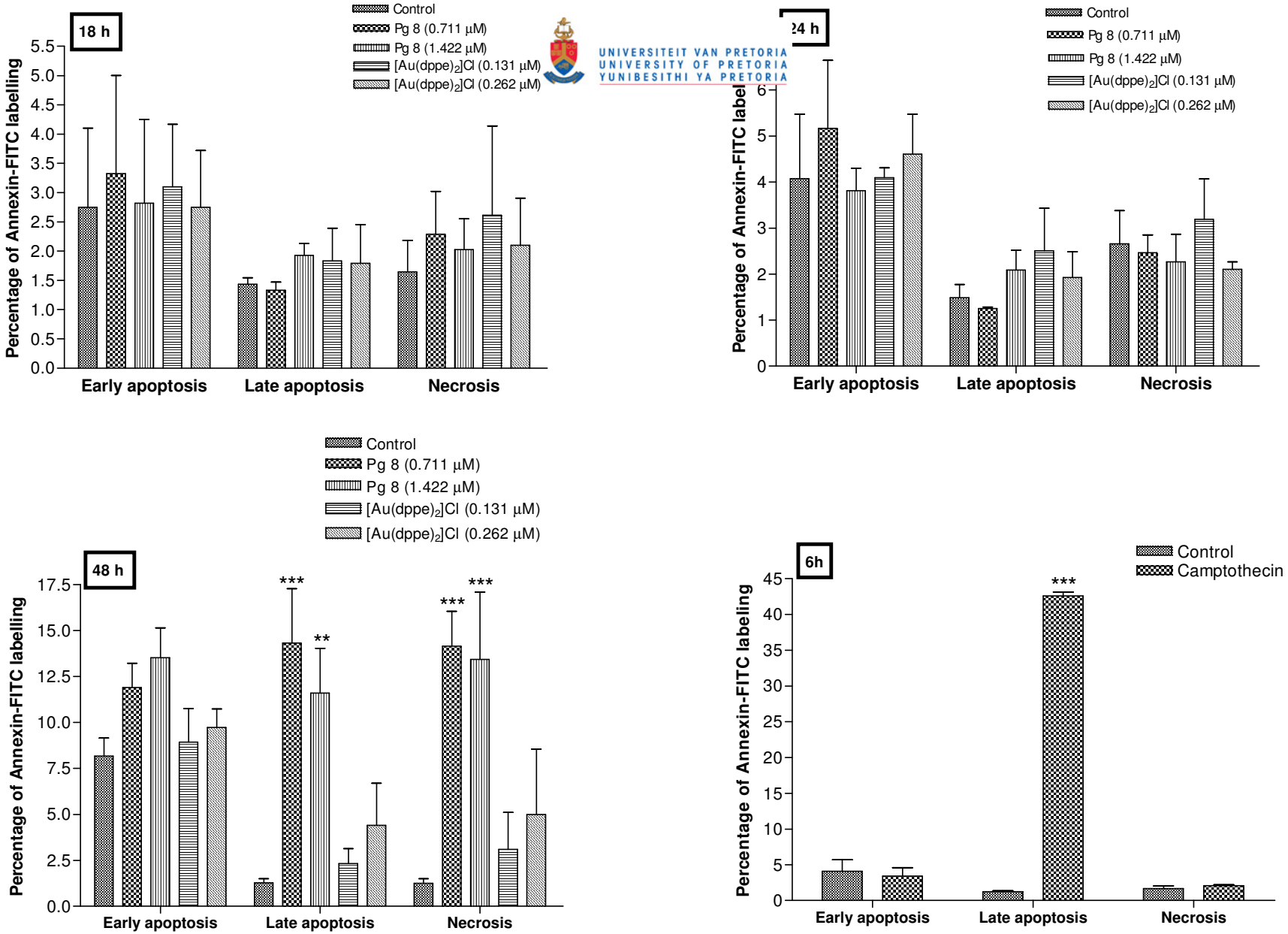

Fig. 7.3: Percentage of Jurkat cells undergoing apoptosis and necrosis after treatment with experimental compounds for 18, 24 and 48 h. The cells treated with camptothecin were incubated for 6h. The data is presented as a mean of three experiments (± S.E.M).

After incubation of Jurkat cells with the compounds for 18 and 24 h, no significant differences were noted between the untreated and the treated groups as between 85 and 90% of cells were viable. However, after exposure of the cells for 48 h, significant differences were observed. Untreated cells had an average of 85% of cells in a viable state and only 8% at the early apoptotic stage. $[Au(dppe)_2]Cl$ (0.131 and 0.262 µM) induced apoptosis in 12% of the cells (9% in early apoptosis and 3% in the stage of late apoptosis) while 77% of the cells were still viable. In contrast, **Pg 8** (0.711 and 1.422 µM) significantly induced apoptosis in 25% of the cells while 14% of cells had undergone necrosis. Only 50% of the cells were viable in this group. Unlike **Pg 8** and $[Au(dppe)_2]Cl$, camptothecin (1 µM) induced apoptosis in Jurkat cells within a short time. After incubation for 6h, about 40% of the cells were in the late apoptotic stage. Viable cells were just over 50% while only 2% of the cells were necrotic. DNA topoisomerase I and II inhibitors induce apoptosis in various cell lines and this is due to DNA-protein complex formation stabilised by DNA topoisomerase I inhibitors that ultimately signal the onset of apoptosis (Sané *et al.,* 2004).

The two compounds behaved differently as observed from the histograms (Fig 7.4). $[Au(dppe)_2]Cl$ treated group had more viable cells (77%) and very few in the necrotic stage (~4 %) while **Pg 8** had a lower percentage of viable cells (50%) and most notably a much higher percentage of them in the necrotic stage (14%). This difference is significant as cytotoxicity assays showed that the former drug was more toxic (IC_{50} = 0.131 µM) while **Pg 8** was at least 5 times less toxic (IC_{50} = 0.711 µM) to Jurkat cells. The mode of cell killing differs as $[Au(dppe)_2]Cl$ mainly induced apoptosis while **Pg 8** seemed to induce both apoptosis and necrosis. While the former compound was toxic to lymphocytes (IC_{50} = 0.903 µM), **Pg 8** was not cytotoxic even at 100 µM. This selectivity for cancer cells by the latter compound may be due to this difference in induction of cell death (necrosis vs. apoptosis). However, it is not clear which factors play a role in triggering an apoptotic or necrotic pathway in the different cells (lymphocytes vs. jurkat cells).

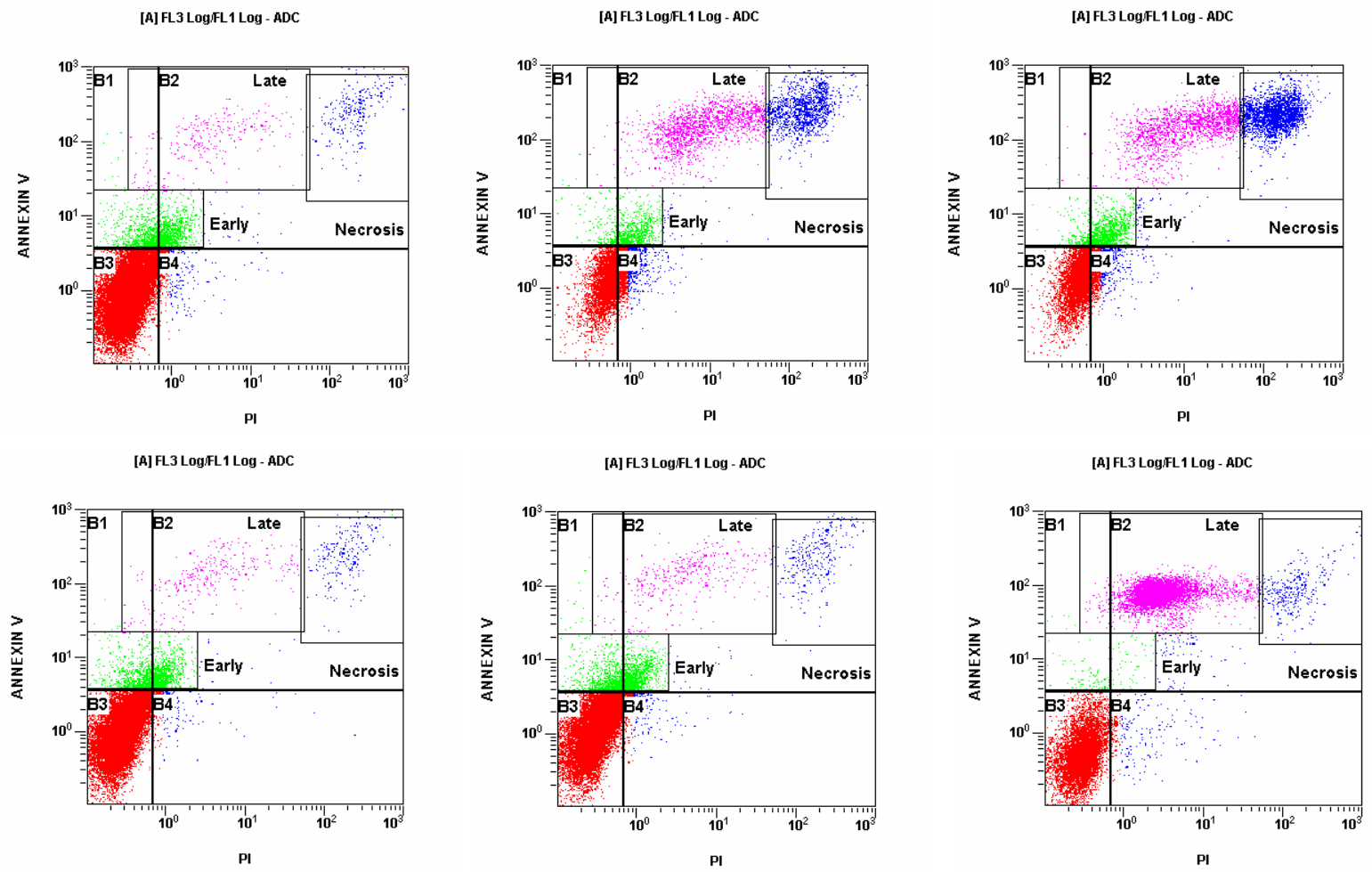

Fig. 7.4: Contour diagram of FITC-Annexin V/PI flow cytometry of Jurkat cells cultured for 48 h with and without experimental compounds. One representative experiment is shown. The top three diagrams (left to right) represent untreated, **Pg 8** (0.711 µM) and **Pg 8** (1.422 µM) while the bottom three diagrams (left to right) represent {[Au(dppe)$_2$]Cl (0.131 µM) and 0.262 µM} and camptothecin (1 µM).

Chemotherapeutic drugs induce damage at a number of different loci, and it is the balance between the pro-apoptotic signals engendered by this damage and survival signals that determines the cellular fate (Makin and Dive, 2001). Various paradigms integrating cytotoxic chemicals and cell death are evolving as pathways become better characterised (Orrenius, 2004). Lethal levels of different toxicants may trigger either apoptotic or necrotic cell death, depending of the cell type and severity of the injury. Further, effectuation of the apoptotic death program requires maintenance of a sufficient intracellular energy level and of a redox state compatible with caspase activation. Thus, ATP depletion or severe oxidative stress may re-direct otherwise apoptotic cell death to necrosis.

A substantial body of recent experimental data suggests that targeting cancer-specific alterations of the apoptotic pathway is an effective strategy to elicit tumour regression *in vivo* (Mashima and Tsuruo, 2005). Further elucidation of the molecular mechanisms of apoptosis in tumour cells and the molecular classification of tumour cells is required to identify an individual strategy to induce selective death to each tumour.